J. Fluid Mech. (1981), *vol.* 113, *pp.* 123–152
Printed in Great Britain

On boundary-layer flow past two-dimensional obstacles

By F. T. SMITH,
Department of Mathematics, Imperial College, London SW7 2BZ
P. W. M. BRIGHTON,† P. S. JACKSON‡ AND J. C. R. HUNT
Department of Applied Mathematics and Theoretical Physics, Silver Street, Cambridge

(Received 10 November 1980)

A complete description is sought for the two-dimensional laminar flow response of an incompressible boundary layer encountering a hump on an otherwise smooth boundary. Given that the typical Reynolds number Re (based on the development length L^* of the boundary layer) is large, the flow characteristics depend on only two parameters, the non-dimensional length and height scales l, h of the obstacle. For short humps of length less than the familiar $O(Re^{-\frac{3}{8}})$ triple-deck size the critical height scale, which produces a nonlinear interaction and hence the prospect of separation, is of order $Re^{-\frac{1}{2}}l^{\frac{1}{4}}$. For long humps whose length is greater than the triple-deck size the corresponding critical height scale is much bigger, of order $l^{\frac{5}{8}}$. Height scales below critical produce only a weak flow response while height scales above critical force relatively large-scale separated motions to occur. In the paper the flow structures and typical solutions produced by two representative cases, a short obstacle of *length* comparable with the oncoming boundary-layer thickness and a long obstacle of *height* comparable with the boundary-layer thickness, are mainly considered. The former case is controlled by the unknown pressure force induced locally in the flow near the hump and by two length scales, that of the hump itself and that of the longer triple deck. The latter case is governed mainly by the inviscid externally produced pressure force. Alternatively, however, all the dominant flow properties in both cases can be obtained as special or limiting solutions of the triple-deck problem. Comparisons between the cases studied are also presented.

1. Introduction

In the theory of the flow past a hump on an otherwise smooth surface there are three independent parameters affecting the motion, even if we concentrate our attention on the steady two-dimensional laminar situation for an incompressible fluid and for a hump that is not too irregular. These three parameters are the Reynolds number and the relative length and thickness scales of the hump. However, for high-Reynolds-number flow theory the present belief is that the character of the motion for any length and height scale hinges about just one principal flow feature, the onset of separation.

† Present address: Applied Mathematics Department, Science Group, Pilkington Brothers Ltd, Research & Development Laboratories, Lathom, Ormskirk, Lancs. L40 5UF.

‡ Present address: Department of Mechanical Engineering, University of Auckland, Auckland, New Zealand.

Accordingly, now that so much more is known (see, for example, the reviews by Stewartson 1974, Messiter 1979 and Smith 1979*c*) about the effects of nonlinearity, and especially of the separation phenomenon, on plane laminar boundary-layer motion it is desirable to attempt a general description for the fundamental flow problem of planar high-Reynolds-number flow past a hump on an otherwise smooth surface. It is supposed that between the effective start and end of the hump its profile is smooth and strictly monotonic on either side of the maximum and has only a single length scale and a single height scale. These two scales rather than the precise shape of the hump then have the overriding influence on the flow response.

There remain some outstanding controversies and uncertainties about the effects of *scale* on the flow of a laminar boundary layer over an isolated two-dimensional hump with small slope on a smooth surface, and in particular controversy about how analyses of humps of different scales match or do not match together. The problem was studied first by Hunt (1971) and Smith (1973). For certain short humps in particular the former adopted a local short-scale approach to study the flow response, whereas the latter suggested a more global long-scale treatment based on triple-deck theory. One of our intentions here is to settle the controversies by presenting a full and clearer account of the flow features produced by a short hump (although long humps will also be analysed: see below). In doing this we will show that the two approaches are in agreement in fact and further that they must both be used, in conjunction, if a complete rational description of the flowfield is to be achieved. For if only the local approach is adopted it fails to cope with the dominant inviscid response of the boundary layer, although it does successfully describe the local viscous wall-layer motion; while application of the triple-deck approach is insufficient for describing all the higher-order effects of the hump, although it does yield the zeroth-order disturbance solution everywhere. Hence a combination of the two approaches is inevitably implied and proves to be a powerful technique for the understanding of the flow past short humps.

The essential physical questions, which we attempt to answer in this paper, are: how do the following flow properties change as the Reynolds number (Re, based on the kinematic viscosity ν^* and the development length L^* of the boundary layer, which determines the boundary thickness δ^*) and the length and thickness (l^*, h^*, where $h^* \leqslant O(l^*)$) of the hump vary? –

(i) Separation. [A phenomenon which occurs on surface-mounted humps of much lower slopes (h^*/l^*) than on similar obstacles in free flows, and which can produce separated flow regions extending many obstacle heights downwind of surface humps.]

(ii) The streamwise velocity over the hump. [Does it increase relative to the velocity at the same height upwind, or decrease, and how far above the hump does the perturbation velocity field extend? In unbounded Couette flows and certain turbulence-modelled flows it increases but in boundary-layer flows over long humps it decreases: what is the explanation?]

(iii) Changes in surface shear stress. [These are much greater than $O(h^*/l^*)$ and decrease downstream at quite different rates depending on l^*.]

(iv) The downstream or wake velocity field. [What kind of humps produce 'wakes' with maximum velocity defects concentrated in narrow surface layers as opposed to those whose wakes have the same order of velocity defect throughout the boundary layer? Are there always integrals which determine the magnitude of these deficits, a point on which Hunt (1971) and Smith (1973) disagreed?]

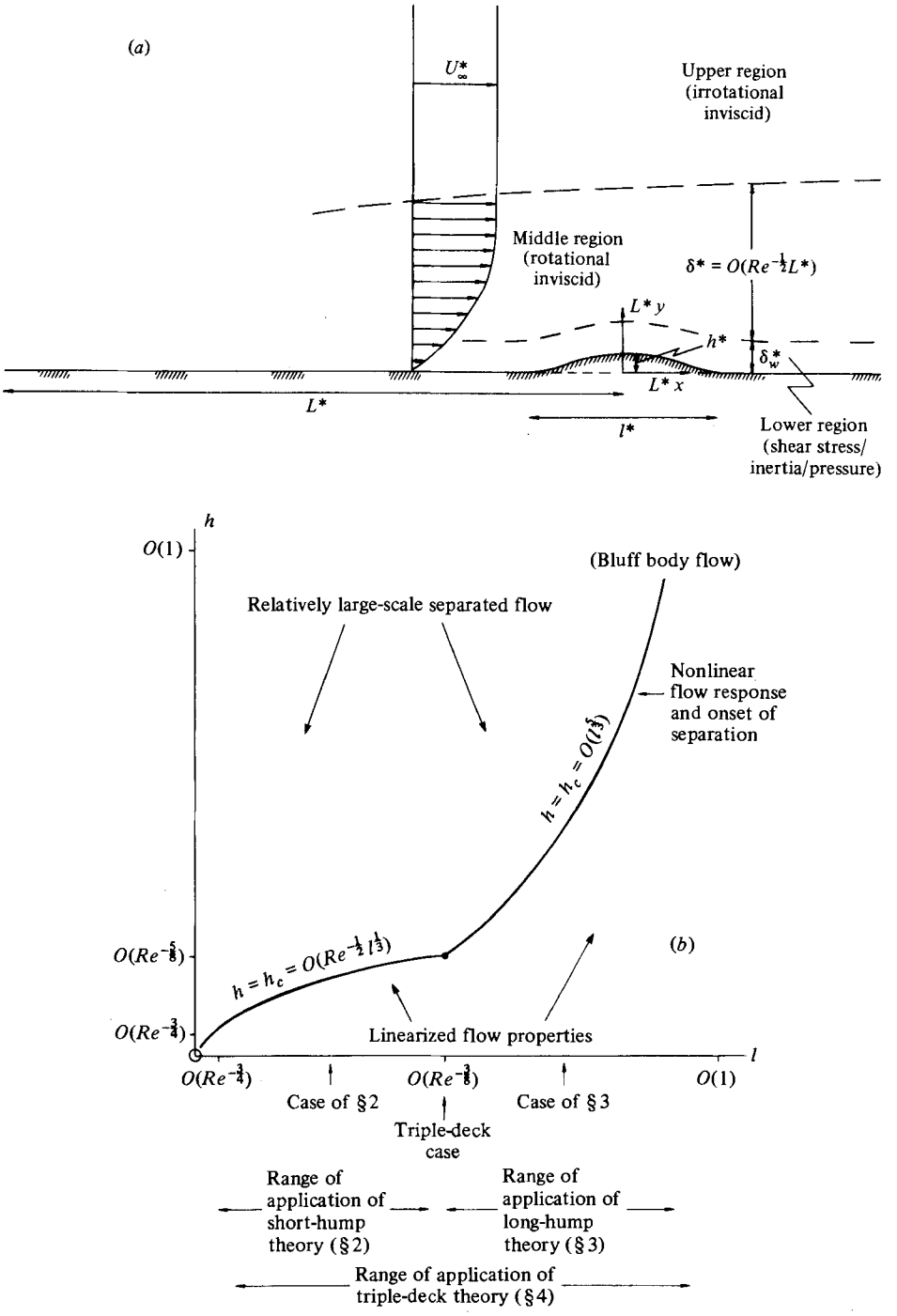

FIGURE 1. (*a*) Definition sketch for the boundary-layer flow over a two-dimensional hump, showing the co-ordinate system, the length scales, the incident velocity profile and the main flow regions. The length scale L^* is chosen so as to be of the same order as the distance from the leading edge of the flat plate in the case of an oncoming Blasius boundary layer. (*b*) The main flow characteristics produced by a hump of height scale h ($=h^*/L^*$) and length scale l ($=l^*/L^*$), and a sketch of the dependence of the critical height scale $h = h_c$ upon the length scale l of the hump. Also shown are the cases studied in §§2, 3 and the triple-deck case, along with the ranges of application of triple-deck theory and of the theories presented in the paper for short humps and for long humps. Smith & Daniels' (1981) work applies above the curve $h = h_c$ but below $h = O(Re^{-\frac{5}{8}})$.

The method of analysis used in this, as in other laminar and turbulence-modelled flow analyses over surface obstacles, is to divide the flow broadly into three regions (figure 1), a lower region (of thickness $\delta_w^* \ll \delta^*$) in which shear stresses balance acceleration and pressure gradients, a middle region with thickness of the order of δ^* and an upper region above the boundary layer. In both the latter regions the perturbations to the incident flow are governed by inviscid dynamics, the difference between the middle and upper regions being that the perturbations there are rotational and irrotational respectively. It is worth reminding those unfamiliar with the jargon that in a 'triple-deck analysis' the flow perturbations have a streamwise length scale L_3^* which is large compared with δ^*. In fact the interactions (described later) between the regions show that $L_3^* = O(Re^{-\frac{3}{8}})\,L^* = O(Re^{\frac{1}{8}})\delta^*$.

In the analysis presented here humps much shorter and longer than L_3^* are considered. For example over the short hump the inviscid middle region has to be broken up into smaller zones where new inviscid properties can develop. An important result of the analysis is to show where and to what accuracy the triple-deck analysis applies to these problems (see figure 1*b*) and where additional analysis is required.

A general analysis for the flow over humps must include at one extreme the flow over a short hump (Hunt 1971; Smith 1973) of low slope whose length is small compared with the boundary-layer thickness, but long enough to induce high-Reynolds-number flow perturbations and whose height is small compared with the viscous shear stress region on the surface; i.e. $(\nu^*/\tau^*)^{\frac{1}{2}} \ll l^* \ll \delta^*$, $h^* \ll l^{*\frac{1}{3}}(\nu^*/\tau^*)^{\frac{1}{3}}$, where τ^* is the incident velocity gradient at the wall; or, in terms normalized on L^* and Re, $Re^{-\frac{3}{4}} \ll l \ll Re^{-\frac{1}{2}}$, $h \ll l^{\frac{1}{3}}Re^{-\frac{1}{2}}$, where $l \equiv l^*/L^*$ and $h \equiv h^*/L^*$ are the relative length and thickness scales of the hump. At the intermediate or triple-deck scale it must include a case analysed by Smith (1973), namely where $l \sim Re^{-\frac{3}{8}}$ and $h \sim l^{\frac{1}{3}}Re^{-\frac{1}{2}}$. Smith argued that an analysis for this case also effectively includes a whole range of short to very long humps, $Re^{-\frac{3}{4}} \ll l \ll O(1)$ – an argument which we find to be correct (§4) in fact, subject to restrictions (e.g. those mentioned in our second paragraph) when higher-order terms are of especial interest. Hunt's (1971) analysis for short humps has similar restrictions on its validity (figure 1*b*). It is because of such restrictions that an analysis extending those of Hunt (1971) and Smith (1973) is necessary. Finally, at the other extreme, for certain very long humps Smith (1973) showed that only a simple though nonlinear displacement effect on the oncoming boundary-layer motion is produced. That result cannot be generally true for all long humps and so again further investigation is necessary to extend the range of understanding of the different flow structures produced by humps of various length and thickness scales.

To handle all the many possible cases and deduce the length scales for such a general analysis we suppose that the relative length ('horizontal') scale l, $\leqslant O(1)$, is given and consider the effects of increasing the relative height ('vertical') scale h of the hump. Then an order-of-magnitude argument soon establishes that the first crucial height reached is $h = h_c = O(l^{\frac{1}{3}}Re^{-\frac{1}{2}})$, since that stage produces a viscous nonlinear response and hence the prospect of separation in the local flow field. For if the height of the viscous wall layer expected near the hump is a fraction δ, say, of the classical oncoming boundary-layer thickness $O(Re^{-\frac{1}{2}})$ then the horizontal velocity component u is of order δ there according to the boundary-layer profile. Hence the inertial and viscous operators are of the orders $\delta l^{-1}(\sim u\,\partial/\partial x)$ and $\delta^{-2}(\sim Re^{-1}\partial^2/\partial y^2)$ respectively and become comparable when $\delta \sim l^{\frac{1}{3}}$. So a hump of height $l^{\frac{1}{3}}Re^{-\frac{1}{2}}$ forces

the analysis of the wall-layer response to be both nonlinear and viscous. Here x, y are the horizontal and vertical co-ordinates non-dimensionalized with respect to L^* while u is measured relative to the local free-stream speed U_∞^* just outside the oncoming boundary layer. For vertical scales $h \ll h_c$ therefore the flow response is purely a linear one; for $h \sim h_c$ it is nonlinear and local separation is a possibility; and for $h \gg h_c$ large-scale breakaway separation (Smith 1977, 1979*a*) and eddy formation, perhaps upstream as well as downstream of the hump, is a distinct prospect. Such a conclusion seems to be warranted for all the cases where $l \leqslant O(Re^{-\frac{3}{8}})$ but for $l \gg O(Re^{-\frac{3}{8}})$ an extra factor comes into play.

For when $l \gg O(Re^{-\frac{3}{8}})$ the viscous nonlinear response arising for $h \sim l^{\frac{1}{3}}Re^{-\frac{1}{2}}$ merely involves a displacement of the entire boundary layer as the whole flow is able simply to lift itself over the hump slowly enough to prevent the occurrence of significant local pressure gradients (as in Smith 1973). Therefore the vertical scale h can be increased safely beyond $h \sim l^{\frac{1}{3}}Re^{-\frac{1}{2}}$ for such long humps without separation being encountered. The pertinent next question then for those cases where $l \gg Re^{-\frac{3}{8}}$ is how far must h be increased beyond $h \sim l^{\frac{1}{3}}Re^{-\frac{1}{2}}$ before separation is encountered? Again the answer stems from an order-of-magnitude argument, although the structure implied is quite different from before. The potential flow outside the boundary layer now responds to the presence of the hump by inducing a pressure variation p of order h/l, i.e. proportional to the hump's typical slope. Here p is non-dimensionalized with respect to $\rho^* U_\infty^{*2}$, where ρ^* is the fluid density. In classical boundary-layer fashion that pressure distribution drives the viscous flow near the hump surface in the thin wall layer which as before has thickness of order $l^{\frac{1}{3}}Re^{-\frac{1}{2}}$ and velocities u of order $\delta \sim l^{\frac{1}{3}}$. Hence the flow response there is nonlinear and so may provoke separation if the inertial and induced pressure forces, $u\partial u/\partial x (\sim \delta^2 l^{-1})$ and $\partial p/\partial x (\sim hl^{-2})$, are comparable, i.e. if $h = O(l^{\frac{5}{3}})$. This suggests the crucial height is $h = h_c \sim l^{\frac{5}{3}}$ whenever $l \gg Re^{-\frac{3}{8}}$.

The intermediate category $l = O(Re^{-\frac{3}{8}})$, the longest one for which the height $h = h_c = O(l^{\frac{1}{3}}Re^{-\frac{1}{2}})$ is still enough to produce separation, therefore defines the shallowest form of hump for which separation can occur and it is of course the triple-deck case. The two different structural forms associated above with (*a*) shorter humps, where $h_c = O(l^{\frac{1}{3}}Re^{-\frac{1}{2}})$ and the pressure response is locally produced, and (*b*) longer humps, where $h_c = O(l^{\frac{5}{3}})$ and the pressure response comes instead from the outer potential flow, amalgamate for the triple-deck length of hump and so lead to the pressure–displacement relation of triple-deck theory. At first sight the triple-deck category therefore seems a very particular one to consider; however it turns out to include the dominant (if not all the) flow features for *all* the other categories mentioned in (*a*) and (*b*) above. A triple-deck study therefore provides the unifying theme between the otherwise disparate flow features arising for shorter and longer humps. It also includes as limiting cases the major flow features for humps so high that $h \gg h_c$ where large-scale separation can occur.

The subdivision of our discussion above, into the three categories of flow past (*a*) shorter humps, (*b*) longer humps and (*c*) the intermediate triple-deck size, forms the basis for the present study. Thus first in § 2 below the category (*a*) is examined. To fix matters there we choose the particular horizontal scale l of the hump to be comparable with the thickness $O(Re^{-\frac{1}{2}})$ of the oncoming boundary layer, although similar flow properties result whenever $Re^{-\frac{3}{4}} \ll l \ll Re^{-\frac{3}{8}}$ (with $h \leqslant O(l^{\frac{1}{3}}Re^{-\frac{1}{2}})$; figure 1*b*). The

solution subdivides then into five main regions of flow, three on the long horizontal scale associated with the triple-deck (§2.1) and two on the short horizontal scale (§2.2) of the hump itself as suggested by Smith (1973) and Hunt (1971) respectively. The various local and wake properties of the short hump case (*a*) are discussed in §§2.3, 2.4. The second category (*b*) is then examined in §3 and, again to fix matters, a specific horizontal scale for the hump is studied, namely $l \sim Re^{-\frac{3}{10}}$ since that produces the interesting case of a longer hump whose height is comparable with the oncoming boundary-layer thickness. Similar flow properties apply whenever $Re^{-\frac{3}{8}} \ll l < O(1)$, with $h \sim l^{\frac{5}{4}}$, however. Comparisons are made, also in §3, between the flow characteristics holding for the categories (*a*) and (*b*). Following that, §4 presents the alternative viewpoint of triple-deck theory. Starting from the nonlinear triple-deck problem associated with (*c*) above the analysis shows that the dominant flow features everywhere for both the categories (*a*), (*b*) of §§2, 3 can be obtained and regarded as limiting or special cases of category (*c*). In anticipation of this last result figure 1(*b*) depicts a summary of the flow properties for humps of various length and height scales. It is believed that by means of the classification (*a*)–(*c*) the present paper provides the characteristics of the flow past any hump whose relative length scale l lies in the range $Re^{-\frac{3}{4}} \ll l \leqslant O(1)$. We note in passing that, for all the categories (*a*)–(*c*) studied in §§2–4 below, the scalings and character of the different regions describing the flow fields can all be derived by the order-of-magnitude arguments put forward earlier in this introduction. Further comparisons of the three cases (*a*)–(*c*) addressed here and consideration of their interrelations are given also in §4. Finally, §5 presents a further discussion and summary.

In the following the Reynolds number is defined by

$$Re = U_\infty^* L^*/\nu^*, \tag{1.1}$$

where ν^* is the kinematic viscosity of the fluid, and v will denote the fluid velocity (non-dimensionalized against U_∞^*) in the y direction. The flow along the smooth surface approaching the hump may be taken to have the local boundary-layer form, to leading order,

$$u = U_B(Y) + O(x), \quad v = O(Re^{-\frac{1}{2}}), \quad p = O(x), \tag{1.2}$$

sufficiently far ahead of the hump if the hump surrounds the origin $x = y = 0$ (figure 1*a*). Here Y is the classical boundary-layer co-ordinate, so that $y = Re^{-\frac{1}{2}}Y$, and the boundary-layer profile $U_B(Y)$ has the properties

$$\left.\begin{aligned} U_B(Y) &\to 1 + O(\exp) \quad \text{as} \quad Y \to \infty, \\ U_B(Y) &\sim \lambda Y + \tfrac{1}{2}\lambda_2 Y^2 \quad \text{as} \quad Y \to 0, \end{aligned}\right\} \tag{1.3}$$

where the given constant $\lambda > 0$ is the local $O(1)$ scaled skin friction of the oncoming boundary layer. Also the constant λ_2 is equal to the local externally produced pressure gradient dp/dx driving the boundary layer in the absence of the hump. An appropriate constant has been added to the pressure to ensure (1.2). In addition we would emphasize our concern here with a rational theory for laminar flow, despite its perhaps limited relevance to real situations. By contrast, turbulence models of (e.g.) wind flow over low hills have been studied by Jackson & Hunt (1975), Counihan, Hunt & Jackson (1974) and Sykes (1981). Again, related studies of the effects of three-dimensionality (Jackson 1973; Smith, Sykes & Brighton 1977; Brighton 1977; Sykes 1980) and of stratification (Sykes 1978) in the flow past humps in boundary layers have also been made.

2. The flow past a short hump

Our task here is to solve the Navier–Stokes equations formally, when $Re \gg 1$, for the flow past a hump of horizontal scale $O(Re^{-\frac{1}{2}})$ and vertical scale $O(Re^{-\frac{3}{8}})$ on the flat plate. Thus the no-slip condition is required on the surface

$$y = \bar{H} Re^{-\frac{3}{8}} F(\bar{x}), \tag{2.1}$$

where $x = Re^{-\frac{1}{2}}\bar{x}$. The dimensionless height factor $\bar{H}$ here can be taken to be $O(1)$ as far as any expansion in terms of the Reynolds number is concerned and for convenience the hump shape $F(\bar{x})$, generally of $O(1)$ for $\bar{x}$ of $O(1)$, is assumed to have finite cross-sectional area, so that

$$f_0 \equiv \int_{-\infty}^{\infty} F(\bar{x})\, d\bar{x} < \infty. \tag{2.2}$$

The main reasons for choosing to concentrate on this particular size of short hump are, first, the importance of the interactions produced by having the hump's length comparable with the oncoming boundary-layer thickness $O(Re^{-\frac{1}{2}})$ and, second, the fact that the height of the hump is just sufficient to provoke a nonlinear response in the local flow including the possibility of separation: see §2.3 below. Again, the choice (2.1) is not quite as restrictive as it may appear at first sight, as will be explained in §§4, 5 below. A diagram representing the asymptotic structure of the main flow regions needed for a complete rational analysis of the present case (2.1) is given in figure 2. As mentioned in §1 there are two distinct streamwise length scales: that of the short hump itself, $x = O(Re^{-\frac{1}{2}})$; and the much longer triple-deck scale, $x = O(Re^{-\frac{3}{8}})$. On the triple-deck scale three regions or decks are produced in the transverse direction: the lower deck ①, the main deck ② and the upper deck ③, with heights $O(Re^{-\frac{5}{8}})$, $O(Re^{-\frac{1}{2}})$ and $O(Re^{-\frac{3}{8}})$ respectively. On the shorter scale of the hump the two major new regions are: the mid-region ④ of the classical boundary-layer height $O(Re^{-\frac{1}{2}})$, and the wall region ⑤ of height $O(Re^{-\frac{3}{8}})$ comparable with the height of the hump (see (2.1)). Lastly, again on the streamwise length scale of the hump there is a rather minor region ⑥ lying between ④ and ⑤ and linking the upstream and downstream portions of the lower deck; ⑥ can largely be ignored, however.

Because of all the disparate length scales involved in the flow over the short hump our discussion will be split into ordered sub-sections below. Thus §2.1 will deal with the interactions arising on the triple-deck length scale, followed by §2.2 where the flow on the hump's length scale will be examined. Then §§2.3, 2.4 will describe the flow properties near and in the various wakes of the hump respectively. It is assumed of course that the motion must resume the boundary-layer form (1.2) sufficiently far from the hump.

2.1. *The triple deck*

The flow properties here are basically the same as in all triple-deck problems (see Stewartson (1974), Messiter (1979)) except that the smallness of the disturbance (2.1) leads to a linear rather than a nonlinear response in the flow field, on the $O(Re^{-\frac{3}{8}})$ length scale involved. Smith's (1973) work gives the order of magnitude and the form of this linear response for a wide range of small humps, and for our particular case (2.1) the following expansions are implied.

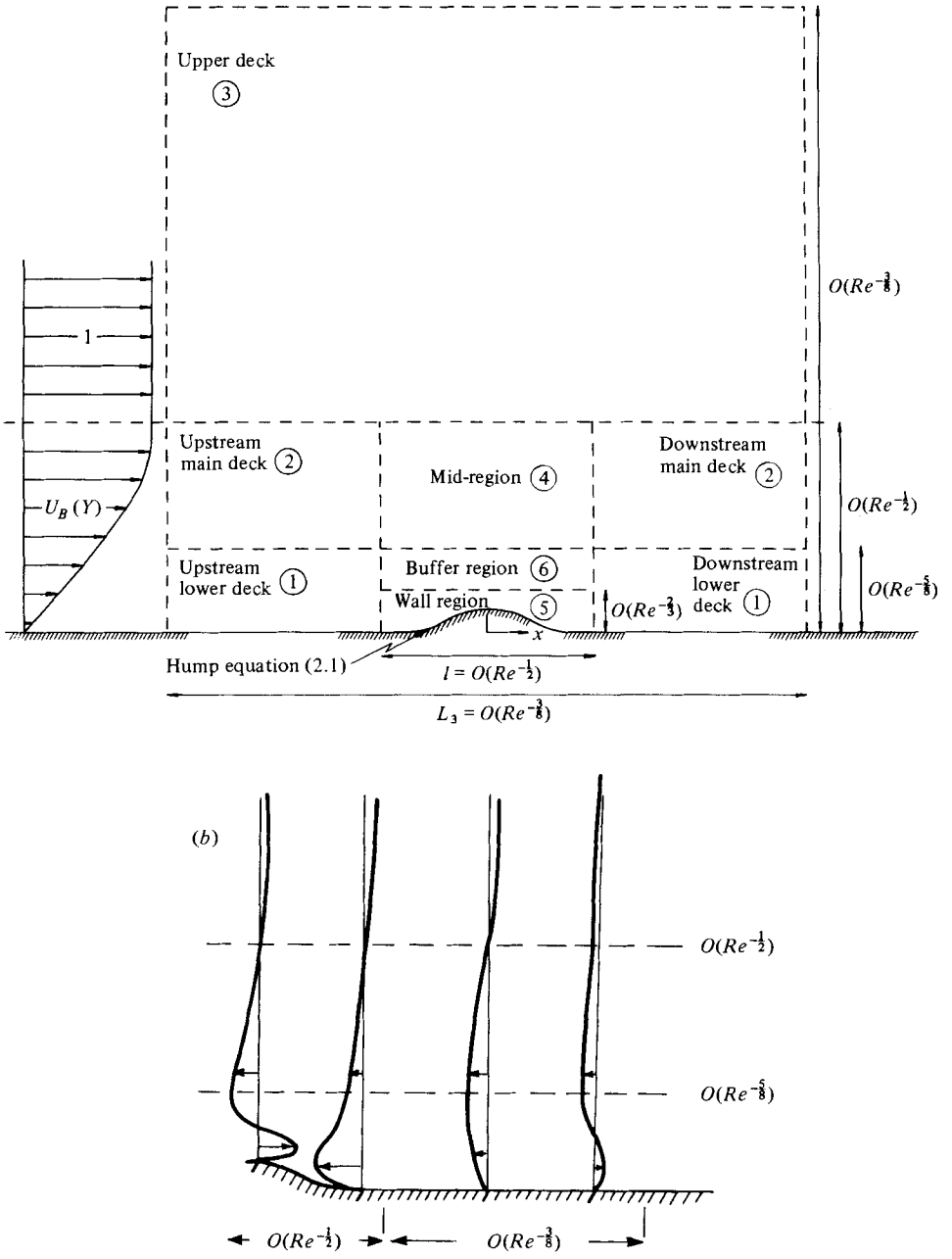

FIGURE 2. Diagrammatical sketch of (*a*) the scales, (*b*) typical velocity profiles of the perturbation velocities in the asymptotic regions ①–⑥ of flow over the short hump studied in §2. Note that in the wall region over the hump the perturbation is relative to the displaced velocity profile $U_B(Y-hF)$ but in the upper regions it is relative to $U_B(Y)$.

In the lower deck, ①:

$$(u, v, p) = (Re^{-\frac{1}{8}}\lambda Z + Re^{-\frac{1}{4}} \times \tfrac{1}{2}\lambda_2 Z^2, 0, Re^{-\frac{3}{8}}\lambda_2 X) + Re^{-\frac{1}{8}}(Re^{-\frac{1}{8}}\bar{U}, Re^{-\frac{3}{8}}\bar{V}, Re^{-\frac{1}{4}}\bar{P}) + \ldots, \quad (2.3a)$$

where $y = Re^{-\frac{5}{8}}Z$.

In the main deck, ②:

$$(u, v, p) = (U_B(Y), 0, Re^{-\frac{3}{8}}\lambda_2 X) + Re^{-\frac{1}{8}}(Re^{-\frac{1}{8}}U_1, Re^{-\frac{1}{4}}V_1, Re^{-\frac{1}{4}}\bar{P}) + \ldots, \quad (2.3b)$$

where $y = Re^{-\frac{1}{8}}Y$.

Here $x = Re^{-\frac{3}{8}}X$ defines the triple-deck co-ordinate X, while the $Re^{-\frac{1}{8}}$ factor in (2.3a, b) is displayed to emphasize the role played by the cross-sectional area ($\propto Re^{-\frac{1}{8}}$ from (2.1)) of the hump relative to the characteristic cross-sectional area of the lower deck (see also (2.5e) and §4 below). Substitution of (2.3b) into the Navier–Stokes equations leads to the familiar forms

$$U_1 = \bar{A}(X)\,U_B'(Y), \quad V_1 = -\bar{A}'(X)\,U_B(Y), \quad \bar{P} = \bar{P}(X), \quad (2.4)$$

representing to leading order a simple displacement of the oncoming boundary-layer profile $U_B(Y)$ with the induced pressure remaining constant across the boundary layer. One relationship between the unknown pressure $\bar{P}$ and displacement $-\bar{A}$ is obtained from the potential flow properties holding in the upper deck ③ outside the boundary layer (Smith 1973; Stewartson 1974):

$$\bar{P}(X) = -\frac{1}{\pi}\int_{-\infty}^{\infty} \frac{\bar{A}'(\xi)\,d\xi}{X-\xi}. \quad (2.5a)$$

The second relationship to fix $\bar{P}$ and $\bar{A}$ stems from the lower-deck flow, for which (2.3a) yields the linearized boundary-layer equations

$$\bar{U}_X + \bar{V}_Z = 0, \quad \lambda Z\bar{U}_X + \lambda\bar{V} = -\bar{P}'(X) + \bar{U}_{ZZ}. \quad (2.5b)$$

These are to be solved in conjunction with the pressure–displacement relation (2.5a) and the conditions

$$(\bar{U}, \bar{V}, \bar{P}, \bar{A}) \to (0, 0, 0, 0) \quad \text{as} \quad X \to \pm\infty, \quad (2.5c)$$

$$\bar{U} \sim \lambda\bar{A}(X) \quad \text{as} \quad Z \to \infty, \quad (2.5d)$$

for matching horizontally with the undisturbed boundary-layer form far upstream and far downstream and vertically with the displaced main deck solution (2.4). The final condition on (2.5b) is the no slip condition

$$\bar{U} = -F_0\,\delta(X) \quad \text{at} \quad Z = 0, \quad (2.5e)$$

obtained by Taylor series expansion and by recognizing that the effect of the short hump (2.1) appears as a delta function on the longer triple-deck scale (Smith 1973) representing an effective hump of total cross-section $F_0 Re^{-\frac{1}{8}}$, the same in the lower-deck co-ordinates (X, Z) as in the more local co-ordinates $(\bar{x}, Y)$ of the mid-region above. The constant F_0, incidentally, is a number depending nonlinearly on $\bar{H}f_0$ in general and is fixed by the shorter-scale problem (2.10a–d) below by means of its asymptote (2.13a–c) (see also §4), although in the special case where $\bar{H}$ is also small $F_0 \sim \bar{H}f_0$ as is noted in §2.4 below.

The solution of (2.5a–e) is obtainable from a Fourier transform and is given by Smith (1973). Its main interest for the concern of this section lies in the behaviour implied for $X \to 0\pm$ since that provides the matching conditions for the motion on the

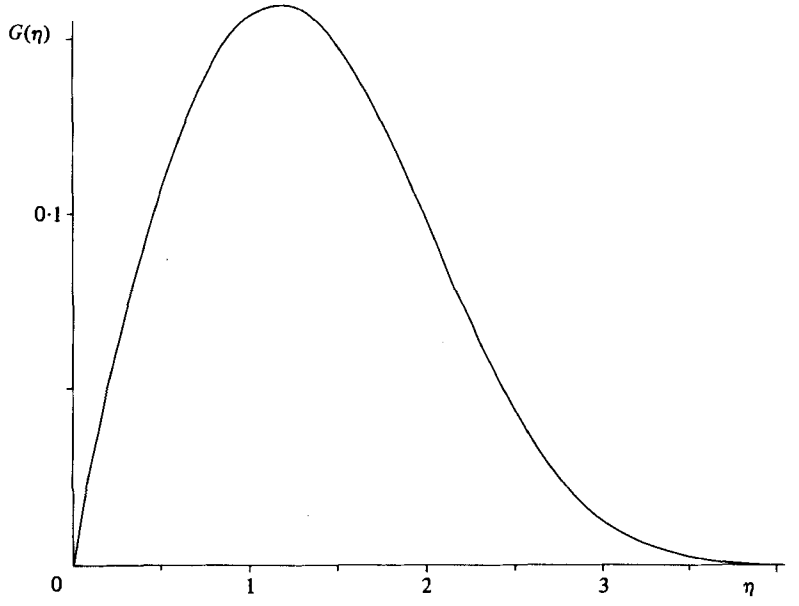

FIGURE 3. Similarity form of the velocity deficit profile in the wall layer downstream of a short hump (the local far-wake, in (2.13*c*)) or at the start of the downstream lower deck (the global near-wake, in (2.6*d*)).

shorter horizontal scale near the hump, i.e. for $\bar{x} \to \pm\infty$. The major properties then are those of the displacement, pressure and surface shear stress

$$\left.\begin{aligned} &\bar{A}(X)/F_0 \sim a_0\lambda^{\frac{5}{4}} + 2a_1\lambda^{\frac{5}{8}}|X|^{\frac{1}{2}} + \dots, \\ &\bar{P}(X)/F_0 \sim b_0\lambda^{\frac{5}{4}} + \dots, \\ &(\partial\bar{U}/\partial Z)_{Z=0}/F_0 \sim O(\ln|X|), \end{aligned}\right\} \quad \text{as} \quad X \to 0-, \tag{2.6a}$$

$$\left.\begin{aligned} &\bar{A}(X)/F_0 \sim a_0\lambda^{\frac{5}{4}} + a_1\lambda^{\frac{5}{8}}X^{\frac{1}{2}} + \dots, \\ &\bar{P}(X)/F_0 \sim b_{-1}\lambda^{\frac{5}{8}}X^{-\frac{2}{3}} + b_0\lambda^{\frac{5}{4}} + \dots, \\ &(\partial\bar{U}/\partial Z)_{Z=0}/F_0 \sim c_{-1}\lambda^{\frac{5}{8}}X^{-\frac{4}{3}} + O(\ln X), \end{aligned}\right\} \quad \text{as} \quad X \to 0+, \tag{2.6b}$$

where

$$a_0 = -3\kappa\cos(\tfrac{1}{8}\pi)/2^{\frac{3}{2}} = -0{\cdot}8106, \quad a_1 = 3\kappa^{\frac{4}{3}}\Gamma(\tfrac{2}{3})/2\pi = 0{\cdot}5020\dots,$$
$$b_{-1} = -\kappa^{\frac{4}{3}}/\Gamma(\tfrac{1}{3}) = -0{\cdot}2898\dots, \quad b_0 = 3\kappa^{\frac{2}{3}}/2^{\frac{5}{2}} = 0{\cdot}4673\dots,$$
$$c_{-1} = -\mathrm{Ai}\,(0)/\Gamma(\tfrac{2}{3}) = -0{\cdot}2622\dots,$$

from Smith (1973) (see, for example, his figure 4) and Brighton (1977). Here $\kappa = (-3\,\mathrm{Ai}'(0))^{\frac{1}{3}} = 0{\cdot}8272\dots$ and Ai is Airy's function. It is found further that the perturbation velocity field $\bar{U}$ leaves a finite non-zero velocity profile over the top of the hump,

$$\left.\begin{aligned} &\bar{U}_0(Z) \equiv \bar{U}(0, Z) \quad \text{at} \quad X = 0 \quad \text{with } Z \text{ fixed} \quad (0 < Z < \infty), \\ &\text{where} \qquad \bar{U}_0(Z) = O(Z) \quad \text{as} \quad Z \to 0+ \end{aligned}\right\} \tag{2.6c}$$

in line with the non-zero value in (2.6*a*) of the displacement $-\bar{A}$ there, but there is a singular behaviour at $Z = 0+$ when $|X| \to 0$, as in all triple-deck or boundary-layer motions incorporating a discontinuity in the wall conditions. Thus in the wake of the obstacle the velocity near the wall is much larger than in (2.6*c*) and develops the similarity form, shown in figure 3,

$$\bar{U}(X, Z) \sim -\lambda F_0 X^{-1} G(\eta) \quad \text{as} \quad X \to 0+ \text{ with } Z = O(X^{\frac{1}{3}}), \tag{2.6d}$$

where $\eta = Z\lambda^{\frac{1}{3}}/X^{\frac{1}{3}}$ and the profile $G(\eta)$ is given by

$$G(\eta) = \frac{1}{2}\left(\frac{\eta^3}{3\pi^3}\right)^{\frac{1}{2}} e^{-\eta^3/18} K_{\frac{1}{6}}(\eta^3/18). \tag{2.6e}$$

The term 'wake' just above refers to the near wake ($X \to 0+$) as far as the triple-deck interaction is concerned and it therefore describes the far wake on the shorter length scale ($\bar{x} = O(1)$) of the hump itself.

The behaviours obtained in (2.6*a–e*) from the flow response for the long triple-deck length scale now enable us to attend immediately to the flow response on that shorter length scale.

2.2. *The more local regions* ④, ⑤, ⑥

In the mid-region ④ $\bar{x}$ and Y are the relevant $O(1)$ co-ordinates and the appropriate expansions, implied by the triple-deck behaviours above, are

$$(u, v, p) = (U_B(Y), 0, 0) + Re^{-\frac{7}{24}}(a_0\lambda^{\frac{1}{4}}F_0\,U_B'(Y), 0, 0) + Re^{-\frac{1}{3}}(U_2, V_2, P_2) + \ldots . \tag{2.7}$$

The dominant perturbation of $O(Re^{-\frac{7}{24}})$ in u here merges with that in (2.3*b*), from (2.4), (2.6*a*), and indeed it is just the continuation of the triple-deck solution. Its independence of $\bar{x}$ stems from the lack of a vertical velocity of the same magnitude in the mid-region which in turn is due to the small efflux from the wall region underneath. The $O(Re^{-\frac{7}{24}})$ contribution therefore represents an eigensolution which depends on the entire long scale response of the triple-deck studied in §2.1 and whose size is greater than that of the main local contribution of order $Re^{-\frac{1}{3}}$ in (2.7). The smaller local contribution is then controlled by the linear equations

$$U_{2\bar{x}} + V_{2Y} = 0, \quad V_{2\bar{x}\bar{x}} + V_{2YY} = \frac{U_B''(Y)}{U_B(Y)} V_2, \tag{2.8}$$

resulting from substitution of (2.7) into the Navier–Stokes equations, by matching constraints upstream, downstream and as $Y \to \infty$, and by the value of the efflux $V_2(\bar{x}, 0+)$ or the wall pressure $P_2(\bar{x}, 0+)$ specified by the solution of the wall region flow beneath. In particular the upper deck ③ demands that the solution of (2.8) should tend to zero as $Y \to \infty$. We note that a Fourier transform of (2.8) leads to Rayleigh's stability equation with zero wave speed and that Lighthill (1957) made an extensive study of (2.8) and its three-dimensional analogue.

The final major zone of flow is the wall region ⑤ close to the hump. For the solution in the intermediate zone ⑥ wherein Z is $O(1)$ again merely requires replacing the term involving $U_B'(Y)$ in (2.8) by the profile $Re^{-\frac{7}{24}}\overline{U}_0(Z)$ defined in (2.6*c*), whilst setting $Y = 0+$ in the $O(Re^{-\frac{1}{3}})$ terms of (2.8). So the major contribution in zone ⑥ is again the triple-deck one forced through (2.6*c*) and there is as yet no interplay between the local effects and the larger more global effects from the triple deck. Then, in the wall region where $\bar{x}$ and z are the appropriate co-ordinates, with $y = Re^{-\frac{3}{8}}z$, the solution expands in the form

$$(u, v, p) = (Re^{-\frac{1}{8}}\tilde{u}, Re^{-\frac{1}{3}}\tilde{v}, Re^{-\frac{1}{3}}\tilde{p}) + \ldots \tag{2.9}$$

as implied by the triple-deck behaviour (2.6*d*) combined with the lower-deck development in (2.3*a*) or, alternatively, by the behaviour of the solutions of (2.8) as $Y \to 0+$ combined with the form of zone ⑥. The flow to lowest order in the wall region therefore brings in the nonlinear boundary-layer equations

$$\tilde{u}_{\bar{x}} + \tilde{v}_z = 0, \quad \tilde{u}\tilde{u}_{\bar{x}} + \tilde{v}\tilde{u}_z = -\tilde{p}_{\bar{x}} + \tilde{u}_{zz}, \quad \tilde{p}_z = 0 \tag{2.10a}$$

with the boundary conditions of no slip at the surface (2.1) and matching upstream and vertically far from the hump:

$$\tilde{u}\begin{cases} = \tilde{v} = 0 \quad \text{on} \quad z = \bar{H}F(\bar{x}), & (2.10b) \\ \to \lambda z \quad \text{as} \quad \bar{x} \to -\infty, & (2.10c) \\ \sim \lambda z + 0 \quad \text{as} \quad z \to \infty. & (2.10d) \end{cases}$$

The outer boundary condition (2.10*d*) on the present short scale should be contrasted with that operative on the longer triple-deck scale, e.g. (2.5*d*). There the horizontal velocity is matched to the displacement solution of the main deck; that non-zero displacement then causes the potential flow in the upper deck which sets up the pressure gradient (2.5*a*); and the latter is precisely the right size of pressure gradient required to drive the lower-deck flow which produced the non-zero displacement in the first place. Here, on the other hand, condition (2.10*d*) means effectively that the leading-order displacement is forced to be zero. Hence the major pressure distribution $\tilde{p}(\bar{x})$ has to be determined as part of the wall region solution alone, separately from and in advance of the flow solution outside. The constraint (2.10*d*) is forced by the elliptic nature of the mid-region flow in (2.7), (2.8) because, as only an efflux of order $Re^{-\frac{1}{8}}$ is consistent with the dimensions of the wall layer, the mid-region equation (2.8) restricts the associated local horizontal velocity to the same order. Alternatively the constraint (2.10*d*) can be regarded as a natural consequence of the earlier triple-deck properties, as §4 below shows. Again, the whole flow structure on the $\bar{x}$ scale has much in common with flows in certain constricted pipes and channels where the same final problem (2.10*a–d*) is met (Smith 1976*a*, *b*).

2.3. *Solutions near the hump*

The crux of the matter now is the solution for the wall region problem (2.10*a–d*), therefore. Fortunately solutions for small and order-one values of $\bar{H}$ can be taken from Smith's (1976*a*, *b*) analysis and calculations: effectively he has $\lambda = \frac{1}{2}$, besides the obvious notational changes and application of Prandtl's transposition theorem. The main comments and points of interest we would note here are the following, taken from Smith (1976*a*, *b*) and also, in linear cases, from Hunt (1971) who derived a linearized form of (2.10*a–d*). First, the pressure distribution is unknown and the displacement known (and zero) in (2.10*a–d*), in contrast with the situation arising in classical boundary-layer theory. Secondly, there is no significant upstream influence at all in the sense that, if $F(\bar{x}) = 0$ for $\bar{x} \leqslant 0$, say, then the solution is the undisturbed boundary-layer form $\tilde{u} - \lambda z = \tilde{v} = \tilde{p} = 0$ for $\bar{x} \leqslant 0$. The only upstream influence in the entire flow field is merely of a linear kind, first on the long triple-deck length scale (§2.1) and then on the short hump length scale, due to the elliptic natures of the upper deck and of the mid-region respectively. Thirdly, numerical solutions for the hump

$$F(\bar{x}) = \bar{x} \exp(-\bar{x}^2/32)\, H(\bar{x}), \qquad (2.11)$$

where $H(\bar{x})$ is the Heaviside step function, are presented by Smith (1976*a*) for various values of $\bar{H}$ including negative ones which correspond to a depression. The reader is referred to figures 5–7 of the last-named paper for graphs of the surface shear stresses, the pressures and a plot of the streamlines within a separation bubble on the leeward slope of a hump. This brings us to the fourth point of interest, which is that any

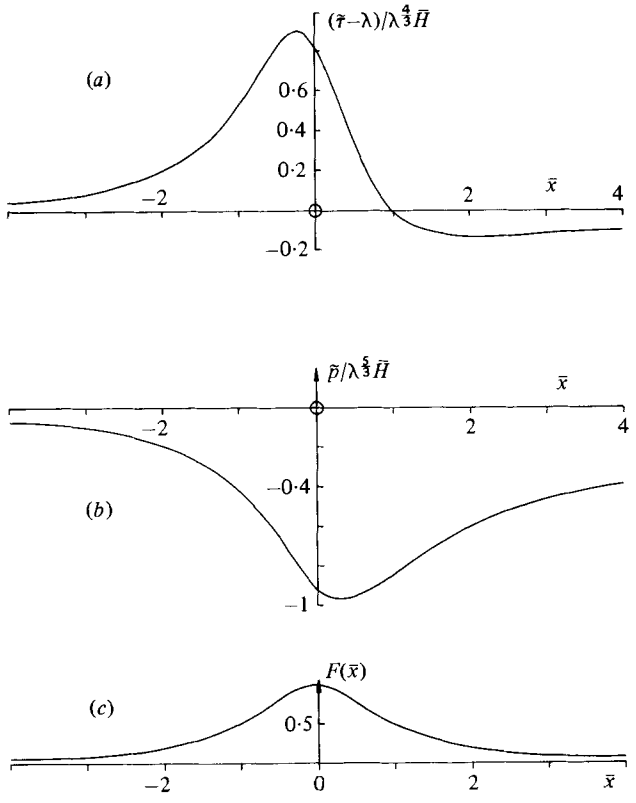

FIGURE 4. Linearized solutions ($\bar{H}$ small) for flow over a short 'Witch of Agnesi' hump (§2): (*a*) Surface shear stress perturbation, $\tilde{\tau} \equiv \tilde{u}_z|_{z=\bar{H}F}$, where $\lambda = U_B'(0)$. (*b*) Pressure distribution. (*c*) Hump shape.

separation in these flows is a regular phenomenon with no breakdown of the boundary-layer equations such as occurs in classical Prandtl boundary-layer theory – the reason is covered by our first comment above. A fifth point is the occurrence of very large increases in the surface shear stress upstream of the peak and the quite slow return to the unperturbed flow conditions downstream (see also §2.4 below). As our sixth remark we note that the linearized solutions of Smith (1976*b*), Hunt (1971), Brighton (1977) for small $\bar{H}$ anticipate well the nonlinear forms of Smith (1976*a*) when $\bar{H}$ is not too large. In particular we present in figure 4 the linearized solution for the case of the Witch of Agnesi,

$$F(\bar{x}) = \frac{1}{(1+\bar{x}^2)}, \tag{2.12}$$

in order to compare the present typical flow properties with those of the flow past the much larger hump studied in the next section and the intermediate size studied in §4. Note that the numerical solutions of Smith (1976*a*) for our flow can be supplemented by a rescaling implicit in his non-dimensionalization. Thus if we know the solution for a given hump in (2.10*b*) then, when the hump's length is stretched by any $O(1)$ length factor q, say, but with its height stretched by the factor $q^{\frac{1}{3}}$, the flow solution is unchanged in essence: we simply multiply $\tilde{u}, \tilde{v}, \tilde{p}, \tilde{x}, z$ by $q^{\frac{1}{3}}, q^{-\frac{1}{3}}, q^{\frac{2}{3}}, q, q^{\frac{1}{3}}$ respectively.

Hence the size of the surface shear stress remains the same. Finally, we note in passing that the case when $\bar{H}$ is large is the subject of a recent study (Smith & Daniels 1981) which shows that the length of the separation bubble then is enormous, as are the induced pressures and surface shear stresses, relative to the scalings contained in (2.9). This last study also includes the removal of Goldstein's (1948) singularity at a classical boundary-layer separation in contrast with the almost certain impossibility of removal, or rather of physically meaningful removal, in larger-scale flows (Stewartson 1970). There is some qualitative similarity at least between Smith & Daniels's theoretical predictions and the experimental findings of Hall (1968), e.g. in his figure 43, of laminar separating regions extending 50 heights downwind of a cylinder on the surface.

2.4. *The various wake properties*

Various processes govern the flow behaviour in the wake of the hump and their interactions are not as simple as might be supposed at first sight. First of course we have the 'locally far wake' of the local response of (2.10*a–d*), i.e. the far wake ($\bar{x} \to +\infty$) on the short $\bar{x}$ scale of §§2.2–2.3 but still the 'globally near wake' ($0 < X \ll 1$) on the longer X scale of §2.1. If the flow of (2.10*a–d*) returns to its original form as $x \to \infty$, which is the suggestion of all the solutions for $\bar{H}$ small, finite or large, then

$$\tilde{u} \sim \lambda z + \tilde{u}'(\bar{x}, z) \quad \text{as} \quad \bar{x} \to +\infty, \tag{2.13a}$$

where, on substitution into (2.10*a*, *b*, *d*) and integration, the velocity deficit $-\tilde{u}'$ satisfies

$$\frac{d}{d\bar{x}}\left[\int_0^\infty z^2 \tilde{u}'(\bar{x}, z)\, dz\right] = 0. \tag{2.13b}$$

This result (cf. (2.15) below) expressing conservation of the integral of the moment of momentum deficit across the wake was also found by Hunt (1971) for the linearized case $\bar{H} \ll 1$, which in fact gives (2.13*b*) directly. Also

$$u'(\bar{x}, z) = -\lambda F_0\, \bar{x}^{-1} G(\eta), \tag{2.13c}$$

where $G(\eta)$ is defined in (2.6*e*), $\eta = z\lambda^{\frac{1}{3}}/\bar{x}^{\frac{1}{3}}$ and the constant F_0 depends in general on the whole numerical solution of (2.10*a–d*), as a remark in §2.1 indicated, although for $\bar{H}$ small $F_0 = \bar{H} f_0$ to leading order. The identity of (2.13*c*) and (2.6*d*) therefore fulfils the matching from the short scale of $\bar{x}$ to the long scale of X, and the locally far wake of (2.13*a–c*) is indeed the same as the globally near wake of (2.6*a–d*). The velocity deficit profile is illustrated in figure 3 and is quite similar to that in a conventional wake away from any wall. Also from (2.13*a–c*) it may be verified that the solution in the mid-region ④ continues into the solution of the main deck ②, as $\bar{x} \to \pm\infty$ in ④ and $X \to 0\pm$ in ②, since the wake entrainment implied by (2.13*a–c*) is given by

$$\lim_{z \to \infty} \tilde{v}(\bar{x}, z) = \tfrac{2}{3} b_{-1} \lambda^{\frac{2}{3}} F_0\, \bar{x}^{-\frac{5}{3}}. \tag{2.13d}$$

Here b_{-1} is given in §2.1 and (2.13*d*) prescribes the value of $V_2(\bar{x}, 0+)$ for zone ④ as $\bar{x} \to \infty$, with $V_2(\bar{x}, 0+) \ll \bar{x}^{-\frac{5}{3}}$ as $\bar{x} \to -\infty$. Hence we find from (2.8) that

$$U_2(\bar{x}, Y) \sim \begin{cases} a_1 \lambda^{\frac{5}{3}} \bar{x}^{\frac{1}{3}} F_0\, U_B'(Y) & \text{as} \quad \bar{x} \to +\infty, \quad (2.14a) \\ 2a_1 \lambda^{\frac{5}{3}} |\bar{x}|^{\frac{1}{3}} F_0\, U_B'(Y) & \text{as} \quad \bar{x} \to -\infty, \quad (2.14b) \end{cases}$$

providing consistency with U_1 in (2.4), using (2.6*a*, *b*) for $\bar{A}(X)$.

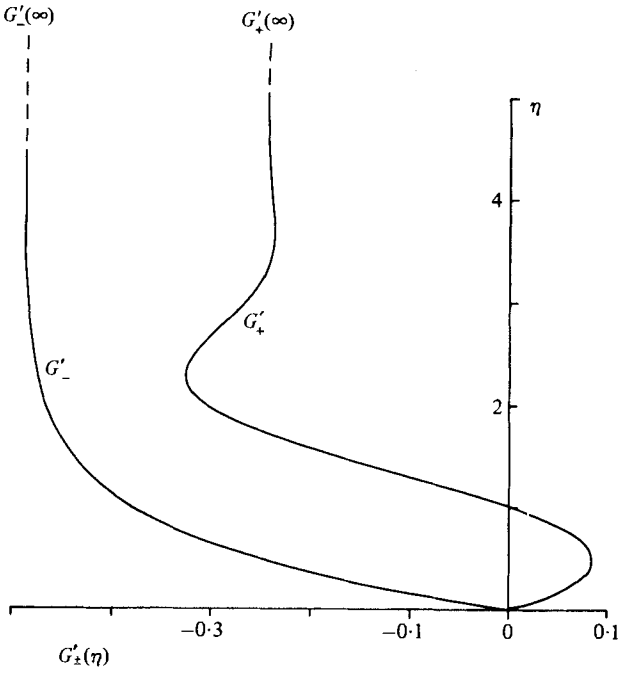

FIGURE 5. Similarity forms of the velocity deficit in the lower deck far upstream of, and in the globally far wake of, the short hump of §2. The same forms also apply far upstream and downstream of the humps considered in §§3, 4, however (see the texts of §§3, 4).

The local wake emerging from the nonlinear response of (2.10*a–d*) i.e. the wake for $\bar{x}$ of order unity with its locally far-wake form in (2.13*a–c*), does not give the nature of the complete wake flow, however. Indeed, as far as the more global length scale of the triple deck is concerned, the locally far wake (2.13*a–c*) is only the start of a new wake process. For the entire motion in §2.1 on the triple-deck length scale is itself the global wake of the hump, for $X > 0$, commencing from the globally near wake in (2.6*b–d*). During the global triple-deck wake $X > 0$ a new balance comes into operation, with the pressure force and the displacement being interrelated through the external potential flow in the upper deck outside the original boundary layer, whereas earlier during the local wake the corresponding displacement is too small to influence the pressure variation. The solution for the global wake is that of §2.1, details of which are given by Smith (1973) (see, for example, his figure 4). The integral condition (2.13*b*) governing the locally far or the globally near wake now becomes invalid as the global wake develops and there seems to be no simple equivalent condition replacing it for the entire global wake. In fact the integral in (2.13*b*) becomes divergent during the global wake because of (2.3*a*), (2.5*d*) and the corresponding result is now

$$\frac{d}{dX}\left[\int_0^\infty Z^2(\bar{U}-\bar{A}(X))\,dZ\right] = -\tfrac{2}{3}\bar{A}(X), \tag{2.15}$$

relating the moment of momentum deficit integral to the displacement, for the entire wake of length $O(Re^{-\frac{3}{8}})$. Only as $X \to 0+$ is the displacement effect $-\bar{A}(X)$ in (2.15) sufficiently small relative to the perturbation velocity that (2.13*b*) can hold. One of the major effects of the new, global, wake interaction with the external flow properties

is an increasing of the rate of decay of the wake properties compared with the forms (2.6*b–d*), i.e. (2.13*a–c*), holding for $X \ll 1$. Thus in particular in the global far wake as $X \to \infty$ or in the global far upstream response as $X \to -\infty$ the perturbation develops the forms (Smith 1973; Jackson 1973)

$$\bar{U} \sim \lambda^{-\frac{2}{3}}|X|^{-\frac{7}{3}}F_0 G'_{\pm}(\eta), \quad \bar{P}(X) \sim F_0/\pi X^2, \quad \eta = Z\lambda^{\frac{1}{3}}/|X|^{\frac{1}{3}}, \tag{2.16a}$$

since there the pressure distribution of (2.5*a*) takes the form associated with a potential dipole at the origin. From (2.5*b–d*) the functions $G_{\pm}$ satisfy

$$G'''_{\pm} \pm \tfrac{1}{3}\eta^2 G''_{\pm} \pm 2\eta G'_{\pm} \mp 2G_{\pm} = \mp \frac{2}{\pi}, \tag{2.16b}$$

with

$$G_{\pm}(0) = G'_{\pm}(0) = 0 = G''_{\pm}(\infty). \tag{2.16c}$$

The solutions are shown in figure 5. Upstream the adverse pressure gradient produces a velocity deficit throughout the boundary layer, whereas downstream the favourable pressure gradient now accelerates the slow-moving fluid near the wall (Smith 1973, equation (4.8)) although away from the wall there is again a velocity deficit. These properties contrast sharply with those of the locally far wake, of (2.13*a–c*) and figure 3, mainly because of the greater importance of the displacement effect here which is responsible *inter alia* for the greatly increased decay ($\propto X^{-\frac{7}{3}}, X^{-2}$) of the velocity and pressure fields compared with those ($\propto X^{-1}, X^{-\frac{2}{3}}$) holding earlier in the locally far wake.

The whole asymptotic structure set out in figure 2 should be self-consistent and the above developments form a basis for a complete rational description of the high-Reynolds-number flow past the hump of (2.1). Next in §3 we discuss the flow due to a long hump on the otherwise smooth surface. Then in §4 the flow features due to both the short and the long humps of this and the next sections are re-examined in the context of triple-deck theory.

3. The flow past a very long hump

In contrast with the study in §2 the present section will concentrate on the flow response due to the presence of a long hump of horizontal length $O(Re^{-\frac{3}{10}})$ and vertical height $O(Re^{-\frac{1}{2}})$ on the plate, for reasons given in the introduction. Thus the wall has the form

$$y = \hat{H} Re^{-\frac{1}{2}} F(\hat{x}), \tag{3.1}$$

say, with $\hat{H}$ of $O(1)$, with $x = Re^{-\frac{3}{10}}\hat{x}$ defining $\hat{x}$ and F defined as in §2. For such a hump the number of distinct regions governing the flow response is at least three but is probably more if, as seems likely in general, separation occurs. Let us develop the solution for attached flow first (figure 6) therefore before addressing briefly the more general case of separated flow.

With the attached flow assumption, the first distinct region of motion on the horizontal scale $\hat{x} = O(1)$ is an outer potential flow zone [1] of vertical scale $O(Re^{-\frac{3}{10}})$, within which the uniform stream $u = 1$, $v = p = 0$ suffers an $O(Re^{-\frac{1}{5}})$ perturbation in view of the characteristic slope or aspect ratio $Re^{-\frac{1}{5}}$ of the hump. So in [1] y is $O(Re^{-\frac{3}{10}})$, $y = Re^{-\frac{3}{10}}\hat{y}$ say, and

$$(u, v, p) = (1, 0, 0) + Re^{-\frac{1}{5}}(\bar{u}_2, \bar{v}_2, \bar{p}_2) + \ldots, \tag{3.2}$$

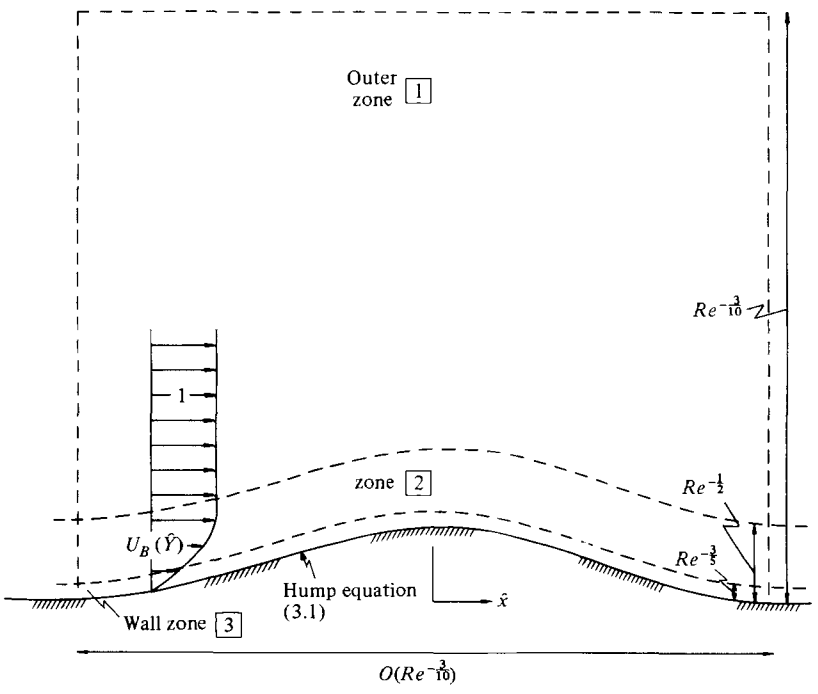

FIGURE 6. Definition sketch of the asymptotic regions 1–3 for the analysis of the boundary-layer flow over the long hump studied in §3. Attached flow is assumed (see §3).

and on substitution into the Navier–Stokes equations we obtain the linearized inviscid potential flow equations for $\bar{u}_2$, $\bar{v}_2$, $\bar{p}_2$. Then in the second zone 2, the main body of the boundary layer, the representation of the flow field is

$$(u, v, p) = (U_B(\hat{Y}), 0, 0) + (Re^{-\frac{1}{10}}\hat{u}, Re^{-\frac{1}{5}}\hat{v}, Re^{-\frac{1}{5}}\hat{p}) + \ldots \tag{3.3}$$

as implied by (3.2) for the pressure and vertical velocity perturbations together with the continuity equation which fixes the order of the horizontal velocity perturbation here. We observe however that the effect on the oncoming boundary-layer profile $U_B(Y)$ is really a nonlinear one, as one would expect from the $O(Re^{-\frac{1}{2}})$ vertical scale of both the hump (3.1) and the boundary layer, although the nonlinearity appears only in the guise of a complete vertical displacement of the oncoming profile since, in (3.3),

$$\hat{Y} = Y - \hat{H}F(\hat{x}). \tag{3.4}$$

The expectation of such an inviscid displacement effect on the motion over the hump (which is now given by $\hat{Y} = 0$) is verified by substitution of (3.3) into the Navier–Stokes equations, yielding the results

$$\hat{v}(\hat{x}, \hat{Y}) = \hat{H}F'(\hat{x})\, U_B(\hat{Y}) \quad \text{and} \quad \hat{p} = \hat{p}(\hat{x}), \tag{3.5}$$

similar to those of Smith (1973, §7). Here (3.5) satisfies not only the continuity and momentum equations to leading order but also the typical inviscid constraint of tangential flow near the wall, $\hat{Y} \to 0+$, since $U_B(\hat{Y}) \to 0+$ there. This last constraint relies heavily on the assumption made of an attached flow description of course. Given the solution (3.5) for the inviscid region 2 we may now return to the outer

potential flow region [1], for the value of the efflux $\hat{v}(\hat{x}, \infty)$ from region [2] supplies one of the boundary conditions on the outer potential flow, namely the equality of $\bar{v}_2(\hat{x}, 0+)$ and $\hat{v}(\hat{x}, \infty)$ or, upon differentiation,

$$-\partial \bar{p}_2/\partial \hat{y}(\hat{x}, 0+) = d\hat{v}(\hat{x}, \infty)/d\hat{x}. \tag{3.6}$$

Use of (3.5), (3.6), together with a boundedness condition in the far field and merging of the pressure between regions [1] and [2], therefore gives the relation

$$\hat{p}(\hat{x}) = \frac{\hat{H}}{\pi} \int_{-\infty}^{\infty} \frac{F'(\xi)\, d\xi}{\hat{x} - \xi} \tag{3.7a}$$

from the outer potential flow. Hence (3.7*a*) directly fixes the main pressure variation induced by the given hump shape (3.1), while (3.3)–(3.5) directly fix the main displacement of the oncoming boundary layer. The displacement is simply equal to the hump shape itself to leading order, although higher-order effects in (3.3) bring in a relatively small unknown correction to the displacement.

The pressure force of (3.7*a*) has an important effect on the slowly moving fluid near the surface of the hump, in the final distinct zone [3], a viscous wall layer. This layer adjacent to the surface is of thickness $O(Re^{-\frac{3}{8}})$ from an order-of-magnitude argument (§ 1). In it the flow field expands in the form

$$(u, v, p) = (Re^{-\frac{1}{10}}\hat{U}, Re^{-\frac{3}{10}}\hat{H}F'(\hat{x})\,\hat{U} + Re^{-\frac{4}{10}}\hat{V}, Re^{-\frac{1}{5}}\hat{p}) + \ldots,$$

with $y = Re^{-\frac{1}{2}}\hat{H}F(\hat{x}) + Re^{-\frac{3}{5}}\hat{Z}$ (or $\hat{Y} = Re^{-\frac{1}{10}}\hat{Z}$) where $\hat{Z}$ is of order unity. Therefore the flow response in layer [3] is a nonlinear phenomenon, the governing equations being the classical boundary-layer equations

$$\hat{U}_{\hat{x}} + \hat{V}_{\hat{Z}} = 0, \quad \hat{U}\hat{U}_{\hat{x}} + \hat{V}\hat{U}_{\hat{Z}} = -\hat{p}'(x) + \hat{U}_{\hat{Z}\hat{Z}}, \tag{3.7b}$$

where the result $\partial \hat{p}/\partial \hat{Z} = 0$ for the vertical momentum balance and the consequent matching of the pressure with that in zone [2] have been applied. The boundary conditions on (3.7*b*) are

$$\hat{U} = \hat{V} = 0 \quad \text{at} \quad \hat{Z} = 0, \tag{3.7c}$$

$$\hat{U} \to \lambda \hat{Z} \qquad \text{as} \quad \hat{x} \to -\infty, \tag{3.7d}$$

$$\frac{\partial \hat{U}}{\partial \hat{Z}} \to \lambda \quad \text{as} \quad \hat{Z} \to \infty, \tag{3.7e}$$

for no slip at the wall (3.7), for matching upstream to the locally uniform shear of the oncoming boundary-layer form and for matching vertically with the solution (3.3) in zone [2]. Since the pressure force driving the wall-layer flow of (3.7*b*) is known in advance from (3.7*a*) the central viscous problem, (3.7*a–e*), is very much like that occurring in classical Prandtl boundary-layer theory. Indeed it is only the matching constraints (3.7*d*, *e*) that offer the main possibility of a difference from a classical approach applied to the flow past the thin body (3.1). These matching constraints reflect the property that the viscous wall region is buried well inside the displaced original boundary layer because the hump, although relatively long, is nevertheless an abrupt disturbance when viewed on the typical $O(1)$ horizontal scale over which the original boundary-layer motion is developing. So the viscous region is influenced mostly by the local uniform shear of the displaced original velocity profile near the wall. There is little doubt that a classical approach would reproduce our problem

(3.7*a–e*) in a limiting sense, with the relatively abrupt thin disturbance (3.1), since the pressure force driving the viscous layer is induced by the inviscid potential thin-aerofoil solution for the flow past the hump, just as in the classical theory. In the present situation, then, the pressure force is known *a priori* but the viscous-layer displacement, $-\hat{A}(\hat{x})$ say, is an unknown, to be determined from the behaviour (from (3.7*e*)),

$$\hat{U} \sim \lambda(\hat{Z}+\hat{A}(\hat{x})) \quad \text{as} \quad \hat{Z}\to\infty, \tag{3.7e'}$$

developing from (3.7*e*); this should be contrasted with the opposite extreme situation holding for the much smaller hump of §2 where instead the displacement can be prescribed and the pressure variation is the unknown to be determined by the viscous wall-layer motion. The link between these two opposite extremes is explained in §4 below in fact, by means of triple-deck theory where in general *both* the driving pressure and the displacement of the viscous wall layer are unknowns. We note too that the displacement $-\hat{A}(\hat{x})$ gives the first correction of relative order $Re^{-\frac{1}{10}}$ to the main known displacement $\hat{H}F(\hat{x})$ of the inviscid region [2].

However, because of the quasi-classical nature of the present flow structure, our assumption of attached flow is vital. The description (3.7*a–e*) above almost certainly cannot cope with separating flow because with the pressure force known in advance, just as in classical boundary-layer theory, the Goldstein (1948) singularity almost certainly arises at the onset of separation, is believed to be irremovable in any physically meaningful way (Stewartson 1970) and thereby renders the whole assumed structure [1]–[3] illogical. The same inability to deal with separation arises in any classical theory of course but not in the theory of §2 above and of §4 below simply because there the wall pressure is an unknown in the viscous wall-layer flow. In the present situation the question of whether the viscous problem of (3.7*a–e*) has an acceptable, i.e. attached, flow solution or not will be a matter of detailed numerical calculation usually, owing to the nonlinearity involved. Physically the separation singularity would seem most likely to occur in the adverse pressure gradient arising in the lee of a high enough hump but on the other hand one would expect attached flow to be possible for a restricted range of hump shapes $F(\hat{x})$ which are not too high, too irregular or too steep. For instance, the attached flow solution is definitely possible when $\hat{H}$ is asymptotically small, since then the solution of (3.7*a–e*) is obtainable analytically in the form of a small perturbation of the original boundary layer:

$$(\hat{U},\hat{V},\hat{p},\hat{A}) = (\lambda\hat{Z},0,0,0)+\hat{H}(\hat{U}_1,\hat{V}_1,\hat{p}_1,\hat{A}_1)+\ldots. \tag{3.8}$$

This linearizes (3.7*b*) and a Fourier transform allows the solutions for the transforms

$$\hat{U}_{1f}(\omega,\hat{Z}) = \int_{-\infty}^{\infty} \hat{U}_1(\hat{x},\hat{Z})\,e^{-i\omega\hat{x}}\,d\hat{x}, \quad \text{etc.}, \tag{3.9a}$$

to be found (as in Smith 1973) in the forms

$$\hat{U}_{1f} = \frac{-\lambda|\omega|(\lambda i\omega)^{\frac{1}{3}}F_f(\omega)}{\lambda^2\mathrm{Ai}'(0)}\int_0^{\hat{Z}} \mathrm{Ai}\,[(i\omega)^{\frac{1}{3}}Z]\,dZ, \tag{3.9b}$$

$$\hat{p}_{1f}(\omega) = -|\omega|F_f(\omega), \quad \hat{A}_{1f}(\omega) = \frac{-|\omega|(\lambda i\omega)^{\frac{1}{3}}F_f(\omega)}{3\mathrm{Ai}'(0)\lambda^2}. \tag{3.9c}$$

Graphs of the distributions of pressure, wall shear stress perturbation and wall-layer

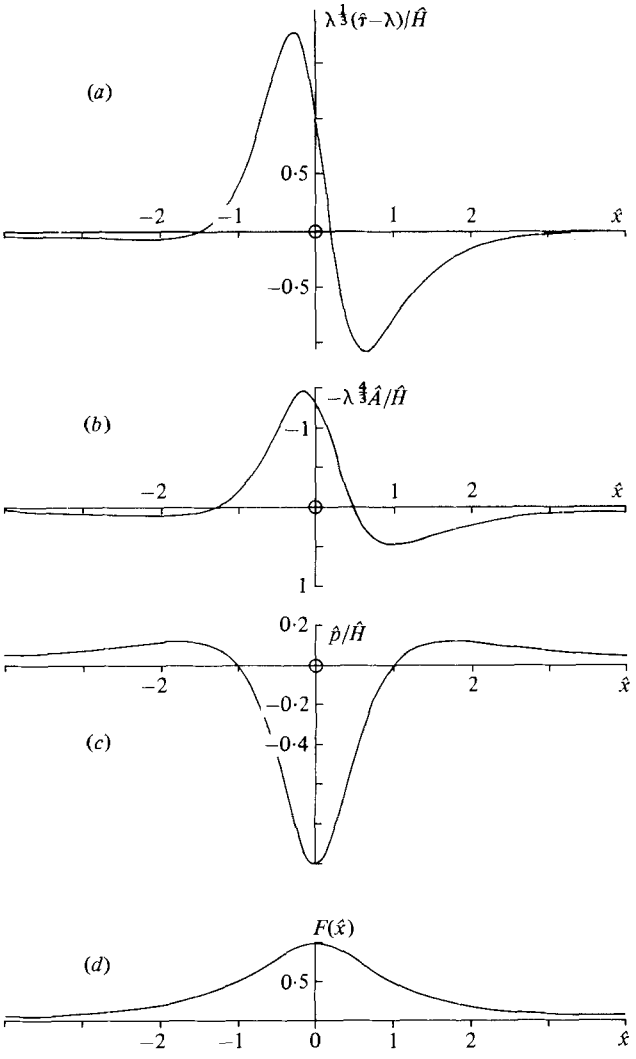

FIGURE 7. Linearized solutions ($\hat{H}$ small) for flow over a long 'Witch of Agnesi' hump (§3): (*a*) Surface shear stress, $\hat{\tau} \equiv \hat{U}_{\hat{z}}|_{\hat{z}=0}$. (*b*) Displacement. (*c*) Pressure. (*d*) Hump shape.

displacement are given in figure 7, again for the case of the Witch of Agnesi $F(\hat{x}) = (1+\hat{x}^2)^{-1}$ as in § 2. Here the wall shear stress displays a peak on the upstream slope of the hump but followed by a reduction of comparable size in the region of adverse pressure gradient beyond the top of the hump. This would suggest the occurrence of the separation singularity there for large enough $\hat{H}$, as would the associated pattern of the displacement. Comparisons of this solution for the longer hump with those for the short hump of § 2 are made later in the paper.

Two final points on the features of the assumed attached flow may now be made. First, a re-scaling similar to that noted in § 2.3 can be used to generate an infinity of solutions from a given nonlinear solution of (3.7*a–e*); it involves multiplying $\hat{U}$, $\hat{V}$, $\hat{p}$, $\hat{A}$, $\hat{x}$, $\hat{Z}$ by $q^{\frac{1}{3}}$, $q^{-\frac{1}{3}}$, $q^{\frac{2}{3}}$, $q^{\frac{1}{3}}$, q, $q^{\frac{1}{3}}$ respectively where q is any $O(1)$ length factor. Second, the upstream influence and the wake of the flow, i.e. the solutions of (3.7*a–e*) for

$\hat{x} \to \mp\infty$ respectively, have just the same forms as in the triple-deck properties of §2.4 above for the globally far wake. Thus the pressure distribution given by (3.7*a*) takes a potential dipole form then and so the velocity profiles far upstream and in the far wake ($\hat{x} \to \mp\infty$) develop the characteristics shown already in figure 5. Further details of these two points are given by Brighton (1977).

If, as seems probable in general, the attached flow assumption made above proves incorrect, then the approach based on [1]–[3] as set out above also becomes incorrect of course. Any separation bubble or eddy is likely to have a height comparable with that of the hump and therefore cannot be described within the context of the thin wall layer [3] above. Instead it exerts a substantial influence, comparable with that of the hump itself, on the entire flow field. The flow structure is obviously more complicated once flow separation is present, then. Nevertheless the structure of such a separated motion is not necessarily far beyond the scope of present theoretical understanding. For it is to be expected that the thin-aerofoil result (3.7*a*) for region [1] still holds, but with the shape $F(x)$ there supplemented by the unknown shape of the separated eddy to give an effective body shape ($F_e(x)$, say) unknown *a priori*. Similarly the inviscid region [2] still has the displaced form of (3.3), although with $F_e(x)$ replacing $F(x)$ again. Then the viscous layer [3] must stay attached to the wall up to separation and thereafter form the thin viscous boundary around the separated eddy or eddies which are presumed to be mainly inviscid. The self-consistent description of the local breakaway separation process here is that of Sychev (1972) and Smith (1977) based on triple-deck theory. Again, although the question concerning the shape of the inviscid eddy is by no means completely settled owing to theoretical difficulties associated with reattachment, a possible candidate for a correct description of the separated flow field is the free-stream-line model of Kirchhoff (1869). This has been studied by Smith (1979*a*, *b*) and Smith & Duck (1980), with regard to the large separated motions occurring in the flow past a bluff body placed in an external stream or in a pipe or channel, and yields good agreement with the reliable numerical evidence available. Some recent numerical work (Fornberg 1980) further supports the free-streamline approach of Smith (1979*a*) for the external flow case, at least as far as Fornberg's work has been checked; the discrepancies suggested by his calculations at higher Reynolds numbers are believed to be illusory in the sense that no reliable checks at all (e.g. on grid sizes or on the approximated boundary conditions) are applied to the calculations then. Accordingly it is envisaged that the free-streamline approach allied to the triple-deck separation process might give a good account of our separated flow field and might even give the correct asymptotic structure replacing that presented above ((3.2)–(3.9)) for attached flow. Some further comments on the separated flow structure are made in the next sections.

4. The triple-deck viewpoint of the hump problems

Let us now reconsider flow past humps in the context of triple-deck theory. This alternative viewpoint (Smith 1973) is that the dominant features of the flow past a vast variety of humps can all be extracted from the nonlinear triple-deck problem; in particular we will verify the validity of that viewpoint for the cases of the short and long humps considered in §§2, 3.

The triple-deck problem is to solve the nonlinear lower deck equations and boundary conditions

$$\begin{cases} U_X + V_Z = 0, \quad UU_X + VU_Z = -P'(X) + U_{ZZ}, & (4.1a) \\ U = V = 0 \quad \text{at} \quad Z = HF(X), & (4.1b) \\ U \sim \lambda(Z + A(X)) \quad \text{as} \quad Z \to \infty, & (4.1c) \\ (U, V, P, A) \to (\lambda Z, 0, 0, 0) \quad \text{as} \quad X \to \pm\infty, & (4.1d) \end{cases}$$

along with the pressure–displacement relation

$$P(X) = -\frac{1}{\pi}\int_{-\infty}^{\infty} \frac{A'(\xi)\,d\xi}{X - \xi}. \tag{4.1e}$$

Here U, V, P represent the velocities and pressure scaled according to the triple-deck laws

$$(u, v, p) = (Re^{-\frac{1}{8}}U, Re^{-\frac{3}{8}}V, Re^{-\frac{1}{4}}P(X)) \tag{4.2}$$

to leading order. Also the hump has the form

$$y = Re^{-\frac{5}{8}}HF(X) \tag{4.3}$$

consistent with the lower-deck size, $O(Re^{-\frac{3}{8}})$ horizontally and $O(Re^{-\frac{5}{8}})$ vertically, defined in §2.1, while H is of order unity formally. Thus (4.1*b*) is the no-slip condition at the surface and (4.1*c*) is the outer matching condition as in §2.1, where $-A(X)$ is the scaled displacement of the main deck.

At first sight the triple-deck case (4.3) seems a specialized one but its use enabled Smith (1973) to deduce some of the properties of both the short and long-scale hump flows of §2.3 above. The advantages of studying the triple-deck case can be put in a more powerful form as follows.

With a view to comparing with §2, consider first the regime $H \ll 1$ but with a hump of short characteristic length $O(H^3)$ on the triple-deck scale X, so that $F(X) \to F(H^3X)$, say, in (4.3). Then the scaling $X = H^3\bar{x}$, $Z = Hz$ are implied immediately together with the expansions

$$(U, V, P, A) = (H\tilde{u}, H^{-1}\tilde{v}, H^2\tilde{p}(\bar{x}), C + H^5\tilde{A}(\bar{x})) + \ldots, \tag{4.4}$$

where C is a constant to be determined. The ordering in powers of H here is chosen to ensure a viscous-inertial-pressure force balance and so substitution of (4.4) into (4.1*a–e*) yields the local problem

$$\tilde{u}_{\bar{x}} + \tilde{v}_z = 0, \quad \tilde{u}\tilde{u}_{\bar{x}} + \tilde{v}\tilde{u}_z = -\tilde{p}'(\bar{x}) + \tilde{u}_{zz}, \tag{4.5a}$$

$$\tilde{u} = \tilde{v} = 0 \quad \text{at} \quad z = F(\bar{x}), \tag{4.5b}$$

$$\tilde{u} \sim \lambda(z + 0) \quad \text{as} \quad z \to \infty, \tag{4.5c}$$

$$\tilde{u} \to \lambda z \quad \text{as} \quad \bar{x} \to -\infty, \tag{4.5d}$$

provided $C \ll H$, which is justified below. Hence we obtain exactly the local viscous wall-layer-flow problem of §2.2, i.e. (2.10*a–d*), with $\bar{H}$ scaled out as referred to in §2.3. This determines the local pressure $\tilde{p}(\bar{x})$ in particular and, unlike the original triple-deck case of (4.1) or the long hump case of §3 and (4.7)–(4.8) below, the pressure–displacement relation (4.1*e*), which becomes

$$\tilde{p}(\bar{x}) = -\frac{1}{\pi}\int_{-\infty}^{\infty} \frac{\tilde{A}'(\xi)\,d\xi}{\bar{x} - \xi} \tag{4.6}$$

now, does *not* determine the local pressure field in the lower layer. Rather, the local pressure determines the relatively small $O(H^5)$ displacement effect in the main part of the boundary layer (indicated by (4.4)) due to the viscous wall layer, a result in line with Hunt's (1971) study. Fortunately, the triple-deck approach (4.1*a–e*) also yields the dominant flow properties in the other four main regions (figure 2) produced by the short hump in §2. For there regions ①–③ are of course the linearized version of (4.1*a–e*), which applies, to a point disturbance, on the $X = O(1)$ scale when H is small and which can be reconciled with that in §2.1 by identifying H with $Re^{-\frac{1}{24}}$ formally† since on the lower-deck scale the present cross-sectional area of the hump is of order H^4 whereas that in §2 is of order $Re^{-\frac{1}{6}}$. Likewise region ④ is dominated by the eigenform of order $Re^{-\frac{7}{24}}$ in (2.7) which is simply the local form of the linearized triple-deck solution anyway. The linearized version shows moreover that C is of order H^4. Therefore in all regions and respects the major features of the flow solution for the shorter case of (2.1) can be achieved in just one step from the triple-deck case.

The same conclusion also applies to the longer case studied in §3. Thus consider the regime $H \gg 1$ but with a hump of large characteristic length $O(H^{\frac{3}{5}})$ on the triple-deck scale X, so that $F(X) \to F(H^{-\frac{3}{5}}X)$. Setting $X = H^{\frac{3}{5}}\hat{x}$ and $Z = HF(\hat{x}) + H^{\frac{1}{5}}\hat{Z}$ then, we expand

$$(U, V, P, A) = (H^{\frac{1}{5}}\hat{U}, H^{\frac{1}{5}}F'(\hat{x})\,\hat{U} + H^{-\frac{1}{5}}\hat{V}, H^{\frac{2}{5}}\hat{p}(\hat{x}), HA_0(\hat{x}) + H^{\frac{1}{5}}\hat{A}(\hat{x})) + \ldots, \tag{4.7}$$

from which we conclude that $A_0(\hat{x}) = -F(\hat{x})$ and hence obtain the controlling equations and boundary conditions

$$\hat{U}_{\hat{x}} + \hat{V}_{\hat{Z}} = 0, \quad \hat{U}\hat{U}_{\hat{x}} + \hat{V}\hat{U}_{\hat{Z}} = -\hat{p}'(\hat{x}) + \hat{U}_{\hat{Z}\hat{Z}}, \tag{4.8a}$$

$$\hat{U} = \hat{V} = 0 \quad \text{at} \quad \hat{Z} = 0, \tag{4.8b}$$

$$\hat{U} \to \lambda\hat{Z} \quad \text{as} \quad \hat{x} \to -\infty, \tag{4.8c}$$

$$\hat{U} \sim \lambda(\hat{Z} + \hat{A}(\hat{x})) \quad \text{as} \quad \hat{Z} \to \infty, \tag{4.8d}$$

from substituting (4.7) into (4.1*a–d*). Also (4.1*e*) becomes now

$$\hat{p}(\hat{x}) = \frac{1}{\pi}\int_{-\infty}^{\infty} \frac{F'(\xi)\,d\xi}{\hat{x} - \xi}. \tag{4.8e}$$

Therefore our problem (4.8*a–e*) is identical with that governing the flow response in §3, i.e. (3.7*a–e*). The other features of §3 can also be gleaned from the triple-deck problem in a like manner, H being identified with $Re^{\frac{1}{5}}$ then.

So each of the long and the short cases of the two previous sections can be accommodated as a special or limiting case of the triple-deck one and is derivable from the latter in one step. Obviously the triple-deck problem unifies the main differences between §2 and §3 since, having the pressure and displacement both unknown but interrelated, the triple deck can allow the feature of zero displacement with unknown

† Strictly severe limitations including $1 \gg H \gg Re^{-N}$ for all $N > 0$ should be placed on H in (4.4), to preserve the complete ordering of the Reynolds-number expansions leading to (4.1*a–e*), but (4.5*a–d*) verify the point that (4.1*a–e*) and (2.10*a–d*) are related limits of the Navier–Stokes equations and indeed only the limitation $1 \gg H \gg Re^{-\frac{1}{6}}$ is required (figure 1*b*) *provided* we concern ourselves with the zeroth-order solution everywhere. Similarly, for §2.3 for example, the limitation on $\bar{H}$ for (2.12) and figure 4 can be slightly extended to $1 \gg \bar{H} \gg Re^{-\frac{1}{12}}$, while (4.7) can be extended to $1 \ll H \ll Re^{\frac{2}{5}}$ (figure 1*b*) as far as the dominant flow solution is concerned.

pressure to emerge for short humps at one extreme (§2) and the feature of known pressure to emerge for very long humps at the other (§3). See also figure 8 below.

5. Further discussion

Certain points of further significance follow on immediately from those of the previous section. First we believe that derivations in §4 of the short- and long-scale flow problems from that of the triple-deck case do help to explain the overwhelming importance of the triple-deck case and why so much attention has been focused on it. For instance the triple-deck problem (4.1*a–e*) contains all the ingredients necessary for a full account of large-scale separated recirculating flows since such an account is expected to emerge when H is large and upstream it would presumably involve the breakaway separation of Smith (1977) which is believed to apply to all such large separations (e.g. Smith 1979*a*). Linearized and/or numerical treatments of (4.1*a–e*) for various values of H have been given by Smith (1973), Napolitano, Davis & Werle (1978) and Sykes (1978), by H. Herwig (private communications, 1979–80) for a depression where $H < 0$, by Dijkstra (1978) for the related problem of flow past a step, and are still under further investigation. The far upstream and downstream (far wake) forms of the flow are given by the behaviours in (2.16*a–c*) incidentally.

A second point is that the importance of the triple-deck solutions should not disguise the fact that if a complete account is required then more regions than those inherent in or stemming from the triple deck are required in general. Thus, in the short-hump case of §2, the mid-region ④, although dominated by the triple-deck eigenform in (2.7), is necessary nevertheless for a full description and appreciation to be gained of the local and global interactions. Only when the local and global approaches, essentially those of Hunt (1971) and Smith (1973), are combined as in §2 can a complete and apparently self-consistent account of the entire flow field be obtained. Indeed, the studies in §§2, 4 are believed to resolve the differences of opinion between the two approaches, showing that each is certainly correct but only in an appropriately limited sense.

Thirdly, for the purposes of completeness and comparison, we present the linearized solution (where $H \ll 1$) of the triple-deck problem (4.1*a–e*). We choose the Witch of Agnesi again but in the form

$$F(X) = \frac{1}{1+(X/q)^2}, \tag{5.1}$$

since the relative length scale factor q here cannot be factored out in the way referred to in §§2, 3. The linearized solution for (5.1) with $H \ll 1$ follows from Smith's (1973) Fourier transform solution and is presented in figure 8. In fact it re-emphasizes some of the points made previously. For figure 8 shows that when q is small the triple-deck solution reproduces the linearized solution of figure 4 for the short hump of §2 and conversely when q is large the linearized solution of figure 7 for the longer hump, studied in §3, is approached. The adjustment that takes place as q increases from $0+$ to ∞, i.e. as the hump's length scale l passes through the triple-deck stage of $O(Re^{-\frac{3}{8}})$, is interesting physically. For when q is small ($l \ll Re^{-\frac{3}{8}}$) the downstream decrease in the shear stress occurs much later, and is much less intense relative to the peak value, than when q is large ($l \gg Re^{-\frac{3}{8}}$). The pressure distributions are also quite

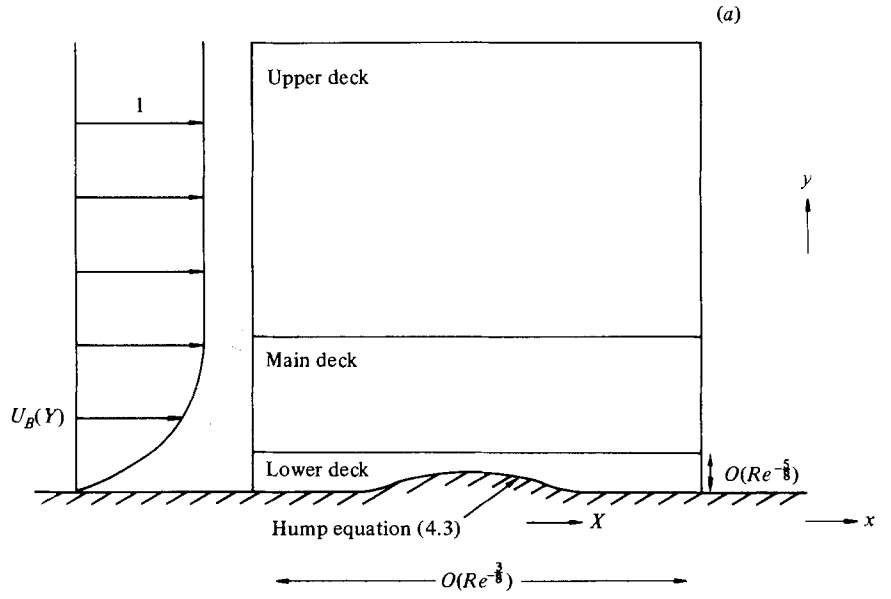

Caption for figure 8*a* on p. 149.

different, with the adverse pressure gradient being milder and spread over a much greater relative distance when q is small. These differences show that when q is small, as in §2, the pressure gradient is not imposed externally but created by the interaction of the inflow into the wake with the incoming vorticity (as in §2 and Hunt 1971); whereas when q is large as in §3 the pressure gradient is in effect imposed externally by the displacement due to the hump shape. The triple-deck solutions for all values of q in figure 8 explain *inter alia* the continuous adjustment from the first to the second form of pressure response and their interrelation.

Fourthly, all the analyses of §§2–4 apply in fact to a wider variety of hump sizes, by use of limiting processes such as those used in (4.4) and (4.7). Indeed, the findings of the present paper and those of Hunt (1971) and Smith (1973) can be summed up in a general description of the effects of a hump's length and height scales (l, h) in fixing the response of the oncoming boundary-layer flow and in particular the onset of separation. It proves advantageous to consider initially humps of length l and height $O(l^{\frac{1}{3}}Re^{-\frac{1}{2}})$. Now for a tiny hump with $l = O(Re^{-\frac{3}{4}})$ the local governing equations remain the full Navier–Stokes equations (Smith 1973; Kiya & Arie 1975; Haussling 1979; see also Sobey 1977) since then $h \sim l^{\frac{1}{3}}Re^{-\frac{1}{2}}$ and l are comparable, while of course if l is less than $O(Re^{-\frac{3}{4}})$ inertialess flow properties may hold which can themselves yield a small though undramatic separation. Next, however, we can conclude that (4.4) describes the main flow features for all values of l greater than $O(Re^{-\frac{3}{4}})$ and less than $O(Re^{-\frac{3}{8}})$, including the particular case $l = O(Re^{-\frac{1}{2}})$ studied in §2. Then the stage $l = O(Re^{-\frac{3}{8}})$ produces the nonlinear triple-deck response (4.1*a–e*), while for l greater than $O(Re^{-\frac{3}{8}})$ but no greater than $O(1)$ we would expect Smith's (1973, §7) simple displacement solution to emerge. By contrast, if the height is less than $O(l^{\frac{1}{3}}Re^{-\frac{1}{2}})$ for a given hump length l then the flow features are merely linearized versions of those just described. But if the height is greater than $O(l^{\frac{1}{3}}Re^{-\frac{1}{2}})$ then major difficulties can (but do not necessarily) arise. The case of §3 is the epitome of this last category at

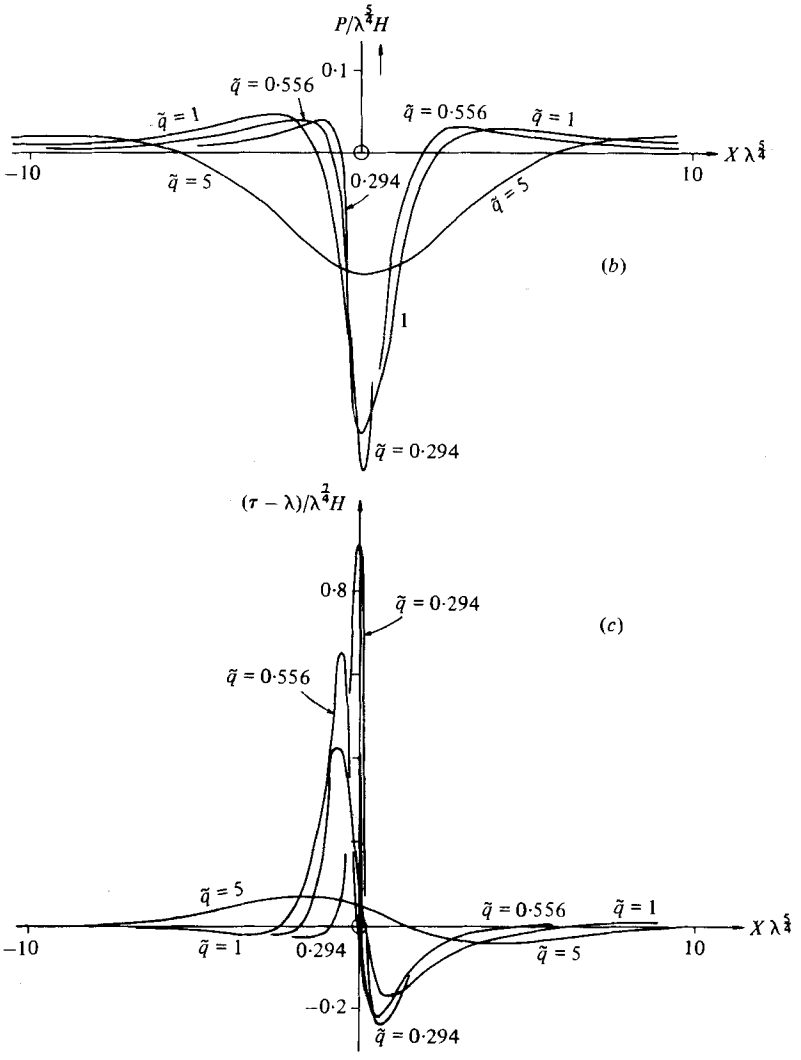

Caption to figures 8*b* and 8*c* on p. 149.

least for the range where l lies between $O(Re^{-\frac{3}{8}})$ and $O(1)$; for in that range the crucial height h is $O(l^{\frac{5}{3}})$ instead of $O(l^{\frac{1}{3}}Re^{-\frac{1}{2}})$.

If the flow remains attached then little doubt surrounds the flow description; but if separation occurs the corresponding flow descriptions must take account of the implications of the triple-deck problem (4.1*a–e*) for large-scale recirculating flows and these implications are still not entirely clear. Clearly, however, the occurrence of separation then does represent a gross change in the character of the fluid motion past the hump, including a recirculatory eddy or eddies of dimensions comparable with or even much larger than those of the hump itself. The other range, where l lies between $O(Re^{-\frac{3}{4}})$ and $O(Re^{-\frac{3}{8}})$, but with h greater than $O(l^{\frac{1}{3}}Re^{-\frac{1}{2}})$, is the subject of Smith & Daniels' (1981) study referred to in §2.3. It is noteworthy also that, for the flow over humps of length scale l in the range $O(Re^{-\frac{3}{4}}) \leqslant l \leqslant O(1)$, the triple-deck scale $l = O(Re^{-\frac{3}{8}})$ gives separation for the smallest size of the aspect ratio,

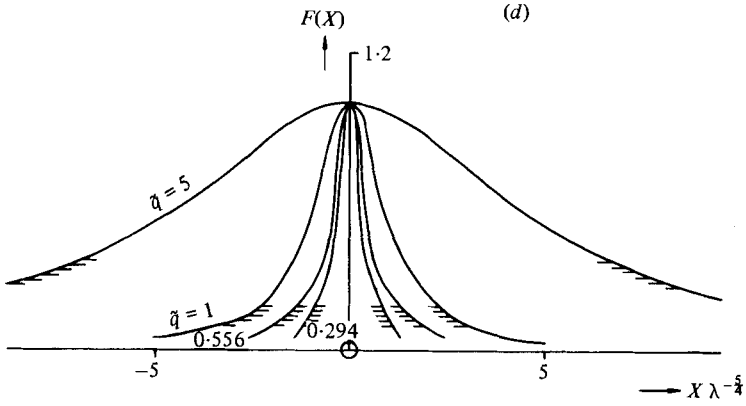

FIGURE 8. (*a*) The triple-deck structure for the intermediate size of hump considered in §§4, 5. (*b*), (*c*) give the linearized solutions (*H* small) for the pressure P and the skin friction $\tau \equiv U_{\hat{Z}}|_{\hat{Z}=HF}$ in the flow over the intermediate Witch of Agnesi, at the values of $\tilde{q} = \lambda^{\frac{5}{4}}q$ shown. (*d*) gives the corresponding hump shapes for each value of the shape factor $\tilde{q}$ ($\tilde{q}$ large or small corresponds to the results for long or short humps in figures 4 and 7 respectively). Note that $(\tau - \lambda)$ is slightly *positive* very far downstream.

$h/l = O(Re^{-\frac{1}{8}})$, while at the ends of the range only obstacles of finite aspect ratio, $h/l = O(1)$, give separation, as demonstrated earlier in figure 1 (*b*).

Concerning the three other flow features listed in §1, viz. the velocity over the hump, the surface shear stress and the wake behaviour, there are also some general physical conclusions (ii)–(iv) below to be drawn from the analysis (see also figure 2).

(ii) For all humps considered here, $O(Re^{-\frac{3}{8}}) \ll l \leqslant O(1)$, in the middle region of the flow (i.e. above the surface region but within the boundary layer) the horizontal velocity component *decreases* relative to its value at the same value of y upstream, i.e. the majority of the boundary layer slows down. This is because the dominant effect (a triple-deck one) is an upward displacement of the incident shear flow streamlines by the hump as well as by the reduced velocity in the surface layer downstream of the hump. Over the short hump this negative displacement perturbation is $O(-U^*_\infty Re^{-\frac{7}{8}} dU_B/dY)$. By contrast the potential-flow-like increase in the velocity produced by flow over the hump and by the flow entrained into the near wake is just smaller and $O(U^*_\infty Re^{-\frac{1}{8}})$. An interesting point is that the former perturbation decreases with height exponentially whereas the latter decreases algebraically ($\propto y^{-\frac{5}{4}}$). So, for a given large value of Re, the latter effect may just possibly be the dominant one in practice over a not insignificant outer part of the boundary layer, if not elsewhere. In the upper region, the largest, outside the boundary layer the perturbation horizontal velocity over the hump always *increases* but the magnitude involved is less than that in the middle region for all ranges of hump length scale. The flow pattern in this region in all cases is the same as potential flow over a surface deformation, whose magnitude is determined by the local flow over the actual hump. For example, over short humps the vertical velocities induced by the hump are $O(Re^{-\frac{1}{8}}U^*_\infty)$ in the outer reaches of the boundary layer; so the horizontal velocities in the upper region are also $O(Re^{-\frac{1}{8}}U^*_\infty)$ or $O(Re^{-\frac{1}{8}}U^*_\infty h/l)$, i.e. less than that of uniform potential flow with velocity U^*_∞ over the hump. In the lowest surface region it is more physically revealing to consider the ratio of local to upstream velocities at the same small displacement height $\hat{y}^* = (y^* - h^*F)$ above the disturbed surface. Then over the summit of the

hump there is always an *increase* in the velocity, at the same value of $\hat{y}^*$. In particular, over the short hump the near-surface velocity there increases by a factor $O(h^*/\delta_w^*)$ or $O(Re^{\frac{1}{8}}h/l)$, as compared with $O(h/l)$ in inviscid fluid flow. Similarly on the downstream or lee side there is a *decrease* in the near-surface velocity by a factor of $O(Re^{\frac{1}{8}}h/l)$. Over the long hump the proportional change in near-surface velocity is $O(h^*/\delta_w^*)$ or $O(Re^{\frac{1}{8}}h/l)$. So the changes in the near-surface velocity due to surface-mounted humps are very much *greater* than the $O(h/l)$ increases in the near-surface velocities in uniform *inviscid* fluid flow over humps. If in either case $h \sim \delta_w$ then separation may occur.

(iii) The lower region results also show how the changes in surface shear stress vary with l/L^*, Re and h/l.

(iv) The wake structure is essentially different for short and very long or intermediate humps (although §4 above can serve to unify all the cases). The former humps first produce a region of large velocity deficit $O(Re^{-\frac{1}{8}}U_\infty^*)$ near the surface much greater than the perturbation in the upper part of the boundary layer, where it is of $O(Re^{-\frac{7}{24}})$ at most. Downstream of longer humps the horizontal velocity perturbation is of the same order in the lower and middle regions of the flow, for example being of $O(Re^{-\frac{7}{24}})$ when $l = O(Re^{-\frac{3}{8}})$, $h = O(Re^{-\frac{5}{8}})$, the intermediate triple-deck scale. Another important difference between flows past short and intermediate humps is that the velocity deficit decays with distance x^* like $(x^*/l^*)^{-1}$ and like $(x^*/l^*)^{-\frac{7}{5}}$ respectively, over a distance $O(l^*)$. However, eventually in the former case when $x^* \gg l^*Re^{\frac{1}{8}}$ the same rapid $x^{-\frac{7}{5}}$ decay sets in as for the longer hump. Again, an adjustment between the integral conditions (2.13*b*) and (2.15) takes place, and it is found that sufficiently far downstream the surface velocity becomes very slightly positive before decaying to zero.

In terms of the dynamics the influence of the short hump does not penetrate strongly enough into the external stream to produce a significant pressure gradient by means of an inviscid interaction. Rather, the flow in the wall layer is determined locally by the diffusion and convection of the incident vorticity whose distribution is distorted directly by the presence of the hump. This is manifested in the parabolic nature of the central problem (2.10*a–d*) and its lack of upstream influence. The pressure gradient may be regarded as being induced by the interplay between the vertical velocities generated in the wall layer and the basic vorticity in the oncoming flow (since as $z \to \infty$ in (2.10*a*) the principal balance is given by $\lambda\tilde{v} \to -d\tilde{p}/d\bar{x}$, as in Hunt (1971)). But on the longer triple-deck length scale the influence of the external stream does become important even for the short hump and it dominates the behaviour further upstream and downstream. Hence the wake in particular has the twofold nature described in §2.4, with the velocity deficit decaying only as $\bar{x}^{-1}$ in the locally far wake (figure 3) but then decaying faster on the triple-deck length scale before finally decaying as $X^{-\frac{7}{5}}$ in the globally far wake (figure 5). By contrast for the longer hump of §3 the physical mechanism of the flow response, if the flow can stay attached, is just that of conventional boundary-layer theory in which a prescribed pressure gradient, given by (3.7*a*), drives the motion. Viscous stresses are confined to the thin wall layer because the length scale of the hump is still much less than the typical length over which the oncoming flow is developing. This mechanism is closely related to the calculational approach of Stratford (1954) and loosely to the turbulence modelling of Jackson & Hunt (1975), but it does not allow for the dramatic effects of

separation on this flow structure, as we have remarked previously. The intermediate size of hump (§4), that of the triple deck, does not suffer the same limitation on the other hand because separation can be allowed. There the apparently distinct physical mechanisms controlling the shorter and longer humps of §§2, 3 are interlinked, so that the distortion of the incident vorticity is controlled in the wall layer (or lower deck) not only by the local presence of the hump but also by the effect of the wall-layer displacement on the external flow. One viewpoint could be that therefore the triple-deck case of (4.1*a–e*) is merely a very special one; but the alternative viewpoint (§4) is that therefore the triple-deck case includes the other two (§§2, 3) as special cases. There is little doubt however that the triple-deck case does hold the key to the large-scale separated-flow properties holding for larger obstacles [e.g. when $O(Re^{-\frac{3}{8}}) \leqslant l \leqslant O(1)$ but with $h \gg l^{\frac{5}{4}}$: see figure 1 (*b*)].

Treatments similar to those above are expected to be applicable to three-dimensional flows also.

One of the practical reasons for analysing laminar flows over surface humps is to provide an exact calculation to guide the development of approximate calculations for turbulence-modelled flows. The analysis presented here confirms that for humps with low slopes ($h^* \ll l^*$), if δ_w^* is the thickness of the lower surface shear stress region and if $h^* \leqslant \delta^*$, then when $l^* \leqslant \delta^*$ (e.g. the short hump) the surface pressure $p_s^* \sim \rho^*(h^*/l^*)\, U_B^*(l^*)\, U_B^*(\delta_w^*)$, where $U_B^*(y^*) = U_\infty^* U_B(Y)$, and the near-surface perturbation velocity *over* the hump at $y^* \sim \delta_w^*$ is $u_s^* \sim (h^*/l^*)\, U_B^*(l^*)$. When $l^* \gg \delta^*$ (e.g. the intermediate and long humps)

$$p_s^* \sim \rho^*(h^*/l^*)\, U_B^*(l^*)^2 \qquad u_s^* \sim (h^*/l^*)\, U_B^*(l^*)^2/U_B^*(\delta_w^*).$$

The latter estimate has been shown by Jackson & Hunt (1975) and Mason & Sykes (1979) to be reasonably accurate for turbulent air flow over hills with slopes as much as $\frac{1}{3}$.

P.W.M.B. is grateful to the Science Research Council, and P.S.J. to a Commonwealth Scholarship, for financial support.

REFERENCES

Brighton, P. W. M. 1977 Ph.D. thesis, University of Cambridge.

Counihan, J., Hunt, J. C. R. & Jackson, P. S. 1974 *J. Fluid Mech.* **64**, 529.

Dijkstra, D. 1978 *Proc. 6th Int. Conf. on Numerical Methods in Fluid Dynamics, Tbilisi, U.S.S.R.*

Fornberg, B. 1980 *J. Fluid Mech.* **98**, 819.

Goldstein, S. 1948 *Quart. J. Mech. Appl. Math.* **1**, 43.

Hall, D. J. 1968 Ph.D. thesis, University of Liverpool.

Haussling, H. J. 1979 *J. Atmos. Sci.* **34**, 589.

Hunt, J. C. R. 1971 *J. Fluid Mech.* **49**, 159.

Jackson, P. S. 1973 Ph.D. thesis, University of Cambridge.

Jackson, P. S. & Hunt, J. C. R. 1975 *Quart. J. Roy. Met. Soc.* **101**, 929.

Kirchhoff, G. 1869 *J. reine angew. Math.* **70**, 289.

Kiya, M. & Arie, M. 1975 *J. Fluid Mech.* **69**, 803.

Lighthill, M. J. 1957 *J. Fluid Mech.* **3**, 113.

Mason, P. J. & Sykes, R. I. 1979 *Quart. J. Roy. Met. Soc.* **105**, 393.

Messiter, A. F. 1979 *Proc. U.S. Appl. Mech. Congr.* 1978, *University of California, Los Angeles.*

NAPOLITANO, M., DAVIS, R. T. & WERLE, M. J. 1978 *A.I.A.A. 11th Fluid & Plasma Dyn. Conf., Seattle*, no. 78-1133.

SMITH, F. T. 1973 *J. Fluid Mech.* **57**, 803.

SMITH, F. T. 1976*a* *Quart. J. Mech. Appl. Math.* **29**, 343.

SMITH, F. T. 1976*b* *Quart. J. Mech. Appl. Math.* **29**, 365.

SMITH, F. T. 1977 *Proc. Roy. Soc.* A **356**, 443.

SMITH, F. T. 1979*a* *J. Fluid Mech.* **92**, 171.

SMITH, F. T. 1979*b* *J. Fluid Mech.* **90**, 725.

SMITH, F. T. 1979*c* Lecture course on 'Theory of Laminar Streaming Flows', presented at C.I.S.M., Udine, Italy, October 1979; also to appear as review in *J. Inst. Math. Applic.* (1981).

SMITH, F. T. & DANIELS, P. G. 1981 *J. Fluid Mech.* **110**, 1.

SMITH, F. T. & DUCK, P. W. 1980 *J. Fluid Mech.* **98**, 727.

SMITH, F. T., SYKES, R. I. & BRIGHTON, P. W. M. 1977 *J. Fluid Mech.* **83**, 163.

SOBEY, I. J. 1977 *J. Fluid Mech.* **83**, 33.

STEWARTSON, K. 1970 *J. Fluid Mech.* **44**, 347.

STEWARTSON, K. 1974 *Advs Appl. Mech.* **14**, 145.

STRATFORD, B. S. 1954 *Aero. Res. Counc. R. & M.* no. 3002.

SYCHEV, V. V. 1972 *Izv. Akad. Nauk S.S.S.R. Mekh. Zhid. i Gaza*, **3**, 47.

SYKES, R. I. 1978 *Proc. Roy. Soc.* A **361**, 225.

SYKES, R. I. 1980 *Proc. Roy. Soc.* A **373**, 311.

SYKES, R. I. 1981 In preparation.